Electromagnetic-Guided Interstitial Catheter Navigation for Gynecological Brachytherapy: a Phase I Trial (E-MINT)

By

Alam Khan

BSc Medical Radiation Sciences, University of Toronto, Canada, 2015

A thesis
presented to Ryerson University
in partial fulfilment of the
requirements for the degree of
Master of Science
in the program of
Biomedical Physics

Toronto, Ontario, Canada, 2020

AUTHOR'S DECLARATION FOR ELECTRONIC SUBMISSION OF A THESIS

I hereby declare that I am the sole author of this thesis. This is a true copy of the thesis, including any required final revisions, as accepted by my examiners.

I authorize Ryerson University to lend this thesis to other institutions or individuals for the purpose of scholarly research.

I further authorize Ryerson University to reproduce this thesis by photocopying or by other means, in total or in part, at the request of other institutions or individuals for the purpose of scholarly research.

I understand that my thesis may be made electronically available to the public.

Abstract

ElectroMagnetic-guided Interstitial catheter Navigation for gynecological brachyTherapy: A Phase I Trial

Alam Khan

Master of Science

Biomedical Physics

Ryerson University

2020

Catheter insertion for gynecological interstitial brachytherapy is a challenging surgical procedure due to the lack of real-time guidance available to Radiation Oncologists. To mitigate the limitations associated with catheter placement, electromagnetic navigation (EMN) was proposed as a solution to the current interstitial brachytherapy workflow. The sequence of events leading up to the completion of this project were as follows, the validation of the system and then the application of the EMN system in a clinical trial. Using a phantom-based validation method, submillimetric accuracy and jitter was characterized for the operational performance of an EMN system in a brachytherapy operating room environment.

Following validation, the EMN system was used for catheter placement in 5 patients, in an ongoing prospective clinical study. The mean catheter deflection documented was 3.52 +/- 2.53 mm when adopting EMN as a form of real-time guidance compared to 5.48 +/- 3.63 mm when the standard clinical workflow (SCW) was employed. The mean catheter spacing when using EMN was 9.31 +/- 4.81 mm compared to 7.09 +/- 6.06 mm when the SCW was followed. Also, the mean intraoperative time was 50.00 +/- 18.80 minutes for EMN and 38.20 +/- 15.29 minutes for the SCW.

The results of this project demonstrate that electromagnetic navigated interstitial catheter placement is promising as a real-time guidance option for the interstitial gynecological brachytherapy workflow.

Acknowledgements

The process of earning my graduate degree has been difficult but rewarding. I would like to thank Dr. Ananth Ravi for his ongoing support throughout my master's, it has been amazing to work under his supervision and gain an understanding of what hard work looks like first hand. Dr. Ananth Ravi is truly a motivating and inspiring individual that I had the privilege to learn from. It was eye opening to see someone who is very academically gifted manoeuver with a very entrepreneurial spirit. Working in the Dr. Ravi research group I came across so many kind and supportive people who assisted me with my research. To name a few, I would especially like to thank Mark Semple, Alexandru Nicoale, and John Dillon for all their help with my project. Also, I would like to thank Dr. James Gräfe , Dr. Carl Kumaradas, Dr. Arman Sarfehnia and Dr. Yuan Xu for being apart of my supervisory committee and oral examining committee.

Aside from academic support, there is no way I would have been able to finish my degree without the endless support provided to me by my loving wife, Sarah Hussein. Even prior to her support in this endeavour, it was she who pushed me to pursue graduate studies and has always had my best interests in mind. Outside of graduate studies, in whatever I am in pursuit of, she has always believed in me. This belief has proven to be invaluable to me as I look to no one else outside of her joyous self for reassurance. In a similar fashion, I would also like to thank my mom, Rukshana Sheikh, for staying by my side regardless of whatever difficulty I introduced into her life when I was growing up as a stubborn child. Not only has she acted as my mother but in a way since my father passed she encompasses both what you would expect from a father figure and a mother figure. Also special thanks to my sister, Jehan Khan, for being like a second mother to me while growing up and continuing to be an amazing sister. Lastly, rest in peace to the greatest of all time, my father, Manzar Ali Khan, with everything I do I just hope to keep his memory alive.

Table of Contents

List of Tables

List of Figures

Acronyms

3D	3-Dimensional
AC	Alternating current
BT	Brachytherapy
CT	Computed tomography
CTV_{HR}	High risk clinical target volume
DOF	Degree of freedom
E-MINT	Electromagnetic-Guided Interstitial Catheter Navigation for brachytherapy
EBRT	External beam radiation therapy
EMN	Electromagnetic navigation
FG	Field generator
FIGO	Federation of Gynecology and Obstetrics
HPV	Human papillomavirus
HDR	High-dose rate
IGABT	Image-guided adaptive brachytherapy
LACC	Locally advanced cervical cancer
MRI	Magnetic resonance imaging
OR	Operating room
P-ISBT	Perineal-based interstitial brachytherapy
SCC	Squamous cell carcinoma
SCW	Standard clinical workflow
SEER	Surveillance, epidemiology, and end results
TRUS	Transrectal ultrasound

Chapter 1 Introduction

1.1 Cervical cancer

The use of electromagnetic navigation for catheter placement in interstitial gynecological brachytherapy is explored in this thesis. Cervical cancer is the most common gynecological cancer and is therefore the disease site of interest throughout this work.

1.1.1 Cervical cancer incidence and mortality

On a global scale, cervical cancer is the fourth most common cancer in women world-wide while in 42 low-resource countries it was the most common cancer in women [55, 57]. According to the World Health Organization, 6.6% of all cancer among women in 2018 were attributed to cervical cancers. Nationally, the Canadian Cancer Society reports that in 2019, 1350 Canadian women will be diagnosed with cervical cancer and an approximated 410 will succumb to the disease. In 2012, an annual incidence of 527 624 new cervical cancer cases and 265 672 cervical cancer-related deaths were documented globally [56]. In 2018, 569 847 new cervical cancer cases and 311 365 deaths from cervical cancer were noted. The increase in incidence and mortality from 2012 to 2018 in cervical cancer occurred despite growth of screening and HPV vaccination in high-income countries [56].

The estimated age-standardized incidence of cervical cancer globally in 2018 was 13.1 per 100 000 women [57]. China and India combined resulted in more than a third of the global cervical cancer burden; there were 106 000 new cases in China, 97 000 new cases in India, 48 000 deaths in China and 60 000 deaths in India [57]. Globally, the mean age at diagnosis of cervical cancer was 53 years old, with a range from 44 years to 68 years old [57]. Cervical cancer was in the leading three cancers affecting women younger than 45 years in 146 of 185 countries assessed in *Figure 1*.

Cervical cancer ranked fourth world-wide for mortality in 2018, with approximately 90% of cervical cancer related deaths occurring in low and middle-income countries [55, 61]. In addition, cervical cancer is the leading cause of cancer death in 42 countries, many of which reside in Sub-Saharan Africa and South Eastern Asia [61]. The global mean age at death from cervical cancer was 59 years

old, with a range from 45 to 76 years old [57].

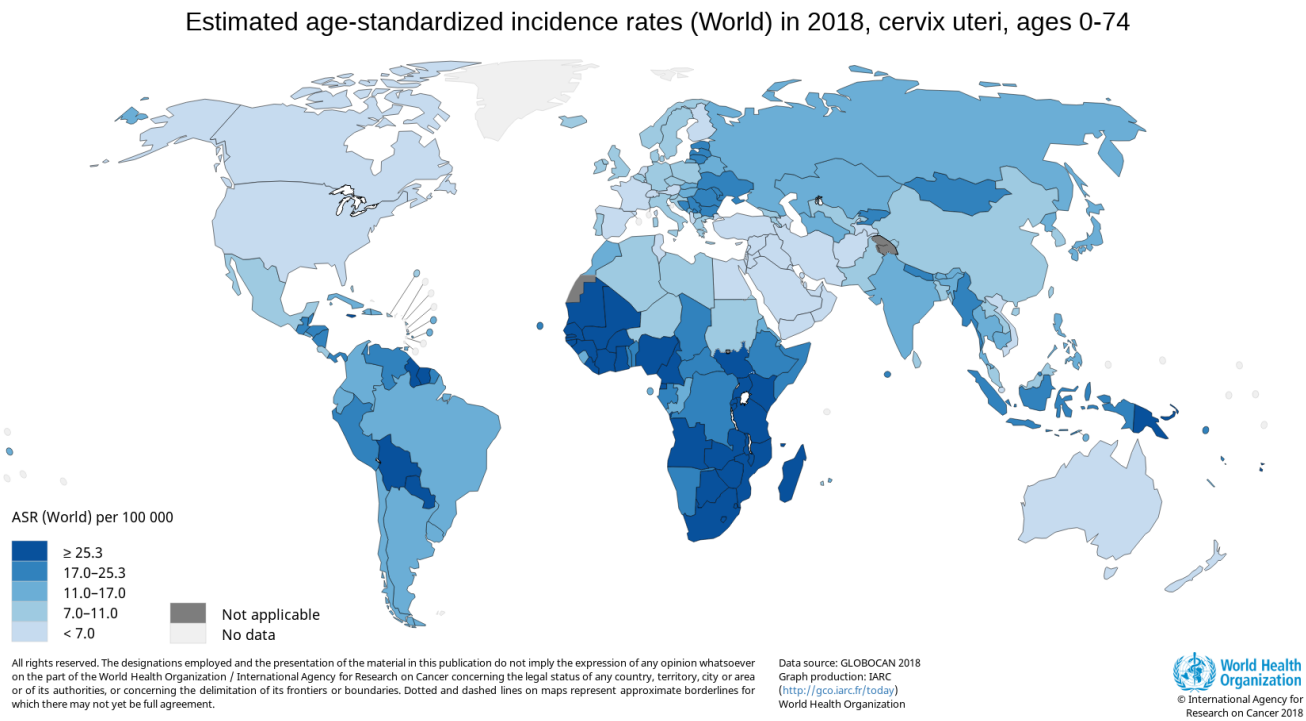

Figure 1. Esimated age-standardized incidence rates globally in 2018 for cervical cancer patients aged 0-74 [7]. The legend title, ASR (World) per 100 000, is the abbreviation for the age-standardzied incidence rates per 100 000 people world wide.

1.1.2 Types of cervical cancer

Two distinctive histologic types of invasive cervical carcinoma are squamous cell carcinomas and adenocarcinomas. Squamous cell carcinomas are cancerous growths found in the exterior layers of the epidermis, which are composed of squamous cells. Adenocarcinomas are cancerous growths that are found in glandular regions. Squamous cell carcinomas (SCC) make up for nearly 80% of all cervical cancers, and adenocarcinoma accounts for the remaining 20% [9].

1.1.2.1 Squamous cell carcinoma

Invasive cervical squamous cell carcinomas are clinically defined by infiltrating nests of neoplastic squamous epithelium in the stroma [60]. The appearance of the nests display microscopically as irregularly and angularly shaped [60]. For cervical cancers, SCC are lesions that arise from the area where squamous cells meet columnar cells in the cervix, this area is termed as the squamocolumnar junction. In addtition to being found in the squamocolumnar junction, SCC may be keratinizing or

non-keratinizing [58,59]. Keratinizing SCC are characterized by cells that are well defined and have large pleomorphic nuclei [60]. Non-keratinizing SCC are defined by the less distinct borders and cytoplasm content that is less in comparison to the keratinizing SCC [60]. SCC have also been associated with improved survival rates in comparison to adenocarcinomas, as indicated by a 833 patient study the 3-year overall survival rates for SCC patients were 85.4% and 75.4% for adenocarcinomas patients [67].

1.1.2.2 Adenocarcinoma

As opposed to SCC, glandular lesions such as adenocarcinomas are sheltered deeper within the canal are less easily detected [9,14]. The adenocarcinoma histologic types are lesions that arise from the endocervix [1]. A defining feature of infiltration by an adenocarcinoma involves either single cells, fragmented glands or partial glands that are lined by malignant cells at a stromal boundary [9]. In addition to declined survival rates, adenocarcinomas, when detected, present a worse prognosis with higher rates of lymph node involvement, and distant metastases when compared to SCC [12].

1.1.3 Risk factors

The majority of cervical carcinomas are linked to human papillomavirus (HPV) [9]. It has been demonstrated that roughly 70% of all cervical cancers are caused by two types of high-risk HPV, type 16 and type 18 [9]. Adenocarcinomas have been linked with HPV type 18 and squamous cell carcinomas have been linked to HPV 16 [15]. A lower incidence of HPV infection is correlated with adenocarcinomas than with squamous cell carcinomas [15]. Additional risk factors of cervical cancer include:

1. Age of first sexual intercourse: Sexual activity beginning at a younger age or close in age to menarche increases the risk of developing cervical cancer. Sexual activity before 18 years of age contributes to a two-time increase in the risk when compared with sexual activity being initiated after 21 years of age [16].
2. Parity: Being younger than 18 years of age at full-term pregnancy, and multiple pregnancies have been identified as risk factors for HPV infection and/or cervical cancer [16].
3. Smoking: Smoking potentially doubles the risk of cervical cancer occurrence when compared with non-smokers. Smoking contributes to a compromised immune system, with the immune system being weakened its ability to fight against HPV infections is affected. The inability to

combat HPV infection increases the likelihood of progression from HPV infection to cervical malignancy [16].

4. Co-infections: An elevated risk of HPV infection is associated with the acquisition of multiple sexually transmitted diseases [16].
5. Extended use of oral contraception: Extended use of oral contraceptives for longer than five years increases the risk of cervical cancer. The risk increases 1.9 times for every five-year increment of oral contraceptive use [16].

1.1.4 Cervical cancer staging

Physical examination for cervical cancer has in the past served as the primary tool for staging and assessment, partially due to lack of accessibility to additional diagnostic resources in many developing nations across the world [17]. In 2018, the staging was amended by the Federation of Gynecology and Obstetrics (FIGO) Gynecologic Oncology Committee to permit medical imaging (ultrasound, CT, MRI) and pathologic findings, where available, to designate the stage [17]. Cervical cancer staging is the most important prognostic factor, followed by nodal status, tumour volume, depth of cervical stromal invasion, and lymphovascular space invasion [17]. The revised staging is shown in *Table 1*.

Table 1. FIGO staging for cervical cancer [17].

Stage	Description
I	The carcinoma is strictly confined to the cervix (extension to the uterine corpus should be disregarded)
IA	Invasive carcinoma that can be diagnosed only by microscopy, with maximum depth of invasion <5 mm
IA1	Measured stromal invasion <3 mm in depth
IA2	Measured stromal invasion ≥3 mm and <5 mm in depth
IB	Invasive carcinoma with measured deepest invasion ≥5 mm (greater than Stage IA), lesion limited to the cervix uteri
IB1	Invasive carcinoma ≥5 mm depth of stromal invasion, and <2 cm in greatest dimension
IB2	Invasive carcinoma ≥2 cm and <4 cm in greatest dimension
IB3	Invasive carcinoma ≥4 cm in greatest dimension
II	The carcinoma invades beyond the uterus, but has not extended onto the lower third of the vagina or to the pelvic wall
IIA	Involvement limited to the upper two-thirds of the vagina without parametrial involvement
IIA1	Invasive carcinoma <4 cm in greatest dimension
IIA2	Invasive carcinoma ≥4 cm in greatest dimension
IIB	With parametrial involvement but not up to the pelvic wall
III	The carcinoma involves the lower third of the vagina and/or extends to the pelvic wall and/or causes hydronephrosis or nonfunctioning kidney and/or involves pelvic and/or para-aortic lymph nodes
IIIA	The carcinoma involves the lower third of the vagina, with no extension to the pelvic wall
IIIB	Extension to the pelvic wall and/or hydronephrosis or nonfunctioning kidney (unless known to be due to another cause)
IIIC	Involvement of pelvic and/or para-aortic lymph nodes, irrespective of tumor size and extent (with r and p notations)
IIIC1	Pelvic lymph node metastasis only
IIIC2	Para-aortic lymph node metastasis
IV	The carcinoma has extended beyond the true pelvis or has involved (biopsy proven) the mucosa of the bladder or rectum. (A bullous edema, as such, does not permit a case to be allotted to Stage IV)
IVA	Spread to adjacent pelvic organs
IVB	Spread to distant organs

1.1.5 Prognosis

Following the completion of concurrent chemoradiotherapy, 5-year overall survival for women with locally advanced cervical cancers (stage IB2 to IVA) is approximately 70% [18]. Prognostic factors that influence overall survival for locally advanced cervical cancers (LACC) include age, race, stage, histological type, grade, lymph node involvement and location, tumour volume, performance status, and the treatment received [18].

1.2 Cervical cancer screening and diagnosis

1.2.1 Cervical cancer screening

Since the introduction of cytology-based screening, cervical cancer incidence and mortality rates have declined by >70% in developed nations, in Canada alone the incidence and mortality rates have declined by 69% and 74%, respectively [62, 65, 66]. The cytology-based test, the Papanicolaou test, involves the viewing of cervical cells fixed on slides. Using a microscope, the slides are examined to determine if the cells are normal or malignant based on their histopathologic features [62]. This test has become the golden standard for cytology-based screening methods and has demonstrated consistent specificity, approximately 98%, with estimates of sensitivity being lower and more variable, approximately 55−80%, for the detection of invasive cancer [62]. The variable sensitivity is accounted for by repeated screening throughout a woman's lifetime [62]. In low-income countries, however, cytology-based screening programs have not been able to achieve the same success as in developed nations [62]. The difficulty in low-income countries is due to the requirements for maintaining cytology based screening programs, the requirements include electricity for microscopes, supplies, and trained cytopathologists to interpret the results of the test [62]. Also, another shortcoming of cytology-based screening in low-resource countries is that for it to be effective it relies on regular screening, which proves difficult for countries without a developed infrastructure for testing [62].

1.2.2 Cervical cancer diagnosis

Upon the determination of abnormalities in cervical cells through cytology-based screening, the diagnosis of stage 1 cervical cancer predominantly relies on the pathologic findings from a biopsy following colposcopy [63]. Colposcopy is a procedure that uses an instrument that is placed close to

the cervical region allowing for the region to be visualized under a high light source [64]. During this procedure, it is necessary to observe the cervical epidermal changes under the action of acetic acid to diagnose the grade of the lesion [64].

The most recent FIGO system encourages the use of imaging to accompany clinical assessment that is based on pathologic findings [22]. Magnetic resonance imaging (MRI) is the golden standard imaging modality for preliminary staging and follow-up of cervical tumours [22]. MRI is an ideal method for assessing primary tumours over 10 mm in size, since it can accurately define tumour size, parametrial invasion, pelvic sidewall invasion, and lymph node metastasis, with up to 95% accuracy for stage IB or higher [22]. In younger patients who want fertility preservation, MRI is necessary for evaluating the possibility of conservative procedures [22].

1.3 Locally advanced cervical cancer treatment

1.3.1 Standard Treatment

The standard treatment for LACC is currently radio-chemotherapy consisting of external beam radiation therapy (EBRT), brachytherapy (BT) and concurrent chemotherapy with Cisplatin [24]. During the last decade, the utilization of MRI guided brachytherapy has expanded based on the Groupe Européen de Curiethérapie and the European Society for Radiotherapy & Oncology (GEC-ESTRO) recommendations [24]. The MRI guidance component includes the acquisition of an MRI at the time of brachytherapy so that treatment volumes are adapted after having received EBRT [24].

1.3.2 Chemotherapy

Concurrent chemotherapy prevents the repair of sublethal damage from radiation, increases the radiosensitivity of cells, and is cytotoxic [72]. The accepted chemotherapy regimen is weekly Cisplatin (40 mg/m^2) unless chemotherapy is prohibited due to patient age and co-morbidity [24]. Reduced chemotherapy dose per cycle is urged when the full dose cannot be administered [24].

1.3.3 External Beam Radiation Therapy

External beam radiation therapy is administered to reduce the amount of disease by targeting the cervix, uterus, superior part of the vagina, parametric tissue, and iliac lymph nodes [71]. The prescribed dose for EBRT is 45 Gy in 25 fractions over the course of 5 weeks [24]. The surveillance,

epidemiology, and end results database was used in a retrospective study performed by Han *et al.* to identify 7359 patients with LACC who completed EBRT with chemotherapy. This work demonstrated that patients who underwent intracavitary BT experienced improved 4-year cause-specific survival and overall survival in comparison to patients who did not undergo BT [69]. The cause-specific survival and overall survival endpoints were measured from the date of diagnosis to the time of death as a result of cervical cancer and to the time of death irrespective of the cause of death, respectively [69]. A 4-year cause-specific survival of 64.3% versus 51.5% and an overall survival rate of 58.2% versus 46.2% was noted for the addition of BT versus without BT [69].

1.3.4 Brachytherapy

Intracavitary brachytherapy is a form of treatment that uses an applicator to introduce radioactive sources into body cavities [77]. The placement of the radiation source nearby the primary tumour allows for the dose to be escalated in the treatment volume while minimizing the dose to critical organs at risk [68, 69]. If achievable, radiobiologically equivalent doses of 90–95 Gy in a 2 Gy per fraction scheme delivered through a combination of EBRT and BT are recommended to maximize local control [116]. A common fractionation scheme for brachytherapy utilized in the treatment of LACC is 7 Gy per fraction, for a total of 4 fractions delivered as 2 fractions per insertion within 48 hours, with the two insertions separated by a week [70].

1.4 Image-guided adaptive brachytherapy

Initially, BT imaging for cervical cancer was two-dimensional (2D) with orthogonal X-rays being the basis for treatment planning [83]. In the early 20th-century, treatment planning approaches were devised by classical brachytherapy schools of thought [91]. The most commonly used system was the Manchester point A system, which involved standard doses prescribed to a fixed point irrespective of tumour size, topography, response to EBRT, and doses to organs at risk (OAR) [91]. To address limitations in treatment planning and imaging, a 3D based approach was developed and termed image-guided adaptive brachytherapy (IGABT) [91]. IGABT is a high-precision radiation treatment that utilizes MRI and/or computed tomography (CT) [8]. The previous 2D based approach was limited in visualizing extensive disease; this is no longer a limitation with MRI and CT imaging. These imaging modalities enable treatment to be individualized with dose adaptation and dose escalation while minimizing dose to OAR [8, 73, 81]. The addition of MRI to brachytherapy

provides a visualization method with superior soft-tissue resolution within the pelvis. Because of this, identification of the cervical tumour extent and the delineation of normal organs is possible. MRI-based BT also makes it possible for complex treatment geometries and three-dimensional volumetric treatment planning with dynamic plan adaptation to account for tumour and OAR changes over time, specifically from the time of diagnosis to the time of BT [73,82]. IGABT with repetitive imaging is a critical component in the treatment of LACC; the use of IGABT is linked with improved overall survival for patients with this disease and is also associated with reduced toxicity [30, 73]. The introduction of IGABT in comparison to conventional brachytherapy methods improved 3-year overall survival for patients with stage IB-IVA cervical cancer, from 51% to 86%, and reduced severe adverse events from 21% to 7% [74].

1.4.1 Combined intracavitary and interstitial brachytherapy

Intracavitary brachytherapy applicators, as seen in *Figure 2 (a)* alone may not sufficiently cover tumour volumes larger than 30 cc [26, 105]. In addition to the size of tumours, tumours involving the parametrium or extension to the pelvic sidewall prove to be challenging to treat with only intracavitary applicators [79]. With these challenges and the advent of IGABT, the classical intracavitary applicators were modified to allow for the use of interstitial catheters to be implanted with the intracavitary component [75]. In a study of 610 LACC patients evaluating the impact of introducing interstitial catheters, it was demonstrated that an improvement of 9 Gy was received by the high-risk clinical target volume (CTV_{HR}) [75]. Also, there was no significant difference in dose to organs at risk between the groups [75]. The 3-year local control rate in patients having a CTV_{HR} volume greater than or equal to 30 cc was 92% in the combined intracavitary and interstitial group compared to 82% in the intracavitary group [75]. Improvement in local control of 2–3% is achieved per 1 Gy increase, hence there is a need for the interstitial component that permits for escalated dose delivery to be achieved with larger than 30 cc treatment volumes [30, 105].

a b

Figure 2. (a) The tandem and ovoid applicator used for intracavitary technique. (b) The Vienna applicator used for combined intracavitary and interstitial technique [105].

The perineal-based interstitial technique, a specialized form of the combined intracavitary interstitial technique, results in high rates of local control with acceptable toxicity, however widespread adoption has been limited [30,84]. The reluctance to adopt this specialized technique is due to its technically challenging nature and concerns of complications from interstitial catheters being inserted through the perineum using the Syed-Neblett template shown in *Figure 3* [26, 30, 104]. Despite reluctance to adopt this technique, IGABT has renewed the interest in the perineal-based interstitial technique [30].

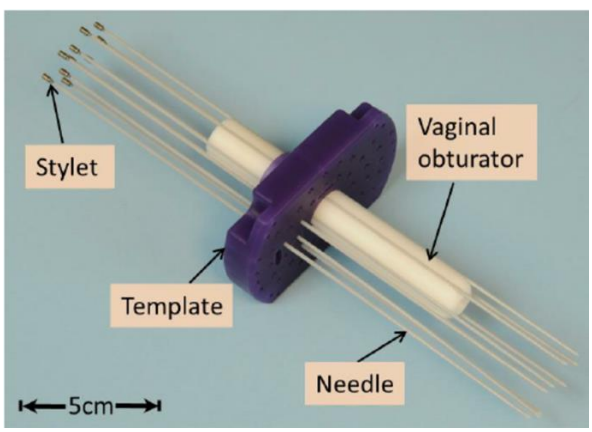

Figure 3. Syed-Neblett template used for perineal-based interstitial technique [104].

To summarize, local control of 85% or greater can be achieved with low treatment related morbidity when taking advantage of IGABT that includes CT and MRI based treatment planning, dose escalation and a combined intracavitary and interstitial brachytherapy technique [75].

1.4.2 Perineal-based interstitial brachytherapy

Perineal-based interstitial brachytherapy (P-ISBT) has been available for over three decades and has been shown to be more effective than standard intracavitary technique in administering dose laterally to large advanced tumours [8]. A local control rate of roughly 80% was associated with the use of perineal interstitial brachytherapy among patients with advanced stage disease [30]. With IGABT, procedural complications from this technique are low and toxicity rates with P-ISBT are similar to the intracavitary alone approach and the standard combined intracavitary interstitial approach [30].

Although IGABT is available, there is still apprehension in performing P-ISBT; in a Canadian survey, only half of the responding centers indicated that they were performing P-ISBT, whereas 96% of them were using IGABT [30, 33]. As such, LACC patients whose tumors would benefit from P-ISBT to improve local control are not receiving this valuable therapeutic option [86]. In addition to concerns about the invasive nature of this procedure, the apprehension is also related to the insertion procedure for catheters into the pelvis, which lacks adequate real-time guidance [28, 86]. Presently, radiation oncologists practicing this technique rely primarily on preoperative imaging to develop baseline treatment plans and then insert catheters clinically [28]. The lack of real-time image guidance brings about concerns that catheters may potentially intrude into unintended organ spaces thereby resulting in severe organ injury and complications, or inadequately coverage of the target volume [28].

While the advantages of P-ISBT have been demonstrated despite patients presenting with several adverse clinical factors such as large tumor size or advanced stage [86], nationwide implementation of this technique is lagging due to the complexity of the clinical workflow, lack of experienced brachytherapy teams and inadequate real-time image guidance [28, 86].

1.4.3 The current workflow for the catheter implantation procedure for P-ISBT

Conventionally, a pre-assessment MRI with a vaginal cylinder inserted is done 1–2 weeks before the treatment for preplanning of needle depths and locations [29]. On the day of the treatment, the patient is anesthetized for the implantation procedure. The procedure is initiated with the placement of the vaginal cylinder, once the cylinder is placed the template is positioned so that it abuts the perineum [29]. When the template is in position, plastic catheters containing metal obturators are implanted

through the template holes [29]. The number, position, and depth of the implanted catheters are based on the physical exam of the patient during the procedure and based on the pre-assessment MRI [29]. After the patient has recovered from anesthesia, imaging is performed using CT and MRI; this imaging is used for treatment planning [29].

The catheter implantation procedure for P-ISBT is based on pre-operative imaging. Real-time guidance needs to incorporated into the implantation procedure for catheters as a supplement to the current workflow. By incorporating real-time guidance into the current workflow, there will be additional confirmation that the catheters are implanted ideally.

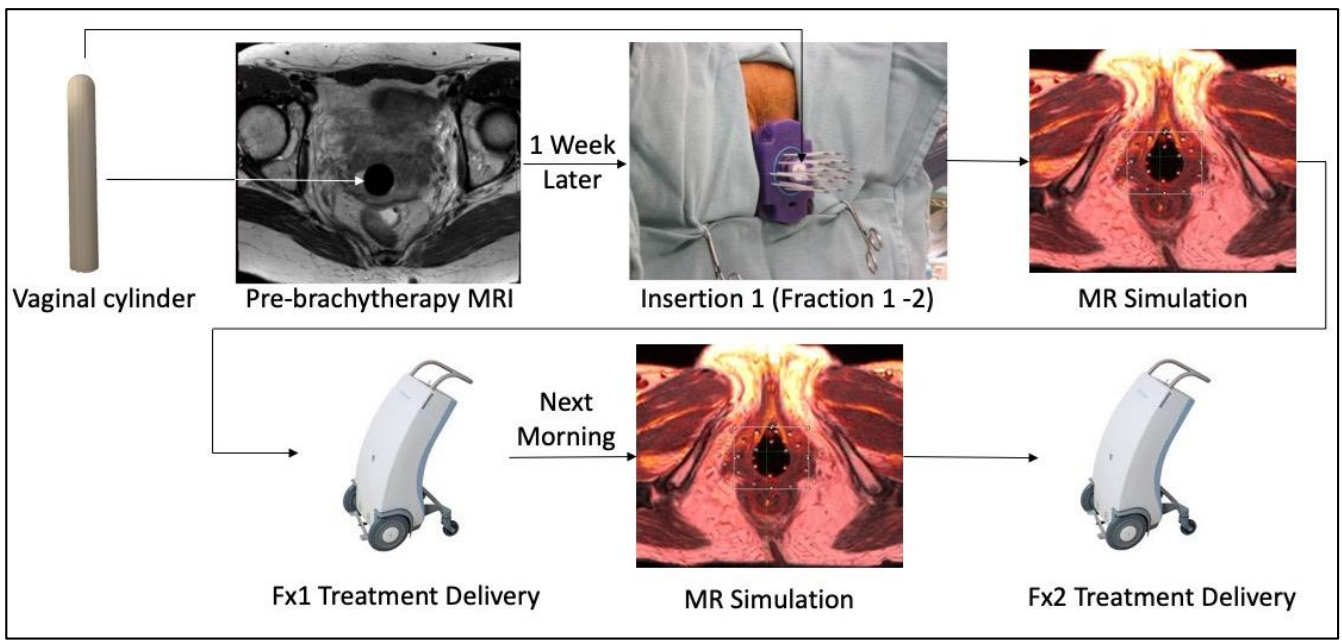

Figure 4. Routine P-ISBT workflow.

1.4 Real-time guidance techniques for P-ISBT implant procedure

1.5.1 Ultrasound

Transrectal ultrasound (TRUS) is the gold standard image guidance technology for real-time imaging of anatomy. TRUS guidance brings the ultrasound probe in closer proximity to the structures of interest [37]. Catheters can be visualized in real-time as they are being implanted in the target volume under direct visualization [37]. Even with the benefits that have been mentioned for TRUS, it is less frequently applied in P-ISBT for LACC primarily due to limitations imposed by anatomy and artefacts [37]. Limitations preventing visualization in this procedure include catheter shadowing

artifacts, organ deformation upon TRUS removal and the vaginal cylinder obstructing the field of view [34].

1.5.2 Magnetic resonance imaging for real-time guidance

Implantation of interstitial brachytherapy catheters under real-time MRI guidance for gynecologic brachytherapy treatment is an active field of study [35]. MRI-guided brachytherapy catheter insertion offers excellent visualization of the tumor and surrounding normal tissue [35]. Accurate placement of catheters potentially improves the homogeneity of dose delivered due to the optimal spacing of catheters, and with the optimal spacing of catheters, fewer catheters need to be placed [38]. Also with accurate catheter placement, there is the possibility of a decline in side effects due to OAR avoidance [38]. More specifically, by preventing the unintentional insertion of a catheter into the bladder or rectum, genitourinary or gastrointestinal toxicities may be decreased [38].

Brigham and Women's Hospital is the only institute to deploy this technique clinically. The interventional MRI suite at this site permits direct access to the patient during the MRI scanning procedure. A pilot study conducted at Brigham and Women's Hospital demonstrated that real-time MRI guidance is feasible in women with gynecologic tumors and assists with the guidance of interstitial catheters [38]. In the same study, P-ISBT under MRI guidance resulted in centimeter-spaced arrangements of catheters with homogenous dose distributions around a clearly depicted tumor volume [38]. The primary limitation of this technique is that there is a heavy resource burden in terms of infrastructure and costs. As such, it has only been implemented at one centre world-wide. In addition, due to the position of the patient within the MR bore it is a strain to place the catheters accurately, making for time-consuming and challenging implantation procedures.

1.5.3 Electromagnetic navigation

1.5.3.1 Application

Electromagnetic navigation (EMN) localizes miniature sensors inside a magnetic field of known geometry, which is created by a field generator (FG) [94]. EMN is presently used for accurate, dose-free, and spatial-temporal localization of sensors in numerous fields of medicine [47]. The primary advantage of EMN is that it can minimize or eliminate the need for real-time radiological imaging [92]. The brachytherapy specific exploration of EMN has involved preclinical studies that use

geometric phantoms to validate EMN systems by characterizing the precision and accuracy of the system in different environments [47]. In a study conducted at the Odette Cancer Centre, the robotic validation of an EMN system resulted in a mean accuracy of <0.5 mm in a non-distorting environment and <1.0 mm in a magnetic field distorting environment [52]. The submillimeter accuracy demonstrated by EMN systems in preclinical studies have indicated that there is potential for the application of EMN in a clinical setting for real-time guidance of catheters in the gynecological P-ISBT workflow [50, 52, 53].

1.5.3.2 Summary of system operation

The principle operation of an EMN system is based on the generation of magnetic fields and the simultaneous tracking of a sensor located within the magnetic fields. The magnetic fields are generated by supplying multiple emitting coils with signals of distinct frequencies [118]. When the sensing coil is placed within the magnetic fields a voltage is induced in the sensor [118]. The induced voltage is a composite signal that is a result of the detection of the magnetic fields generated by all of the emitting coils [118, 119]. The induced voltage includes components that represent each voltage induced in the sensor due to each emitting coil. The components of the induced voltage are separated from one and another by using a Fourier transform to yield a frequency domain representation [119]. The separated components are then used in a non-linear system of equations to determine the position and orientation of the sensor with respect to the emitter coils [119]. *Figure 5* depicts the EMN system framework utilized to generate the position and orientation of a sensor in a tracking volume.

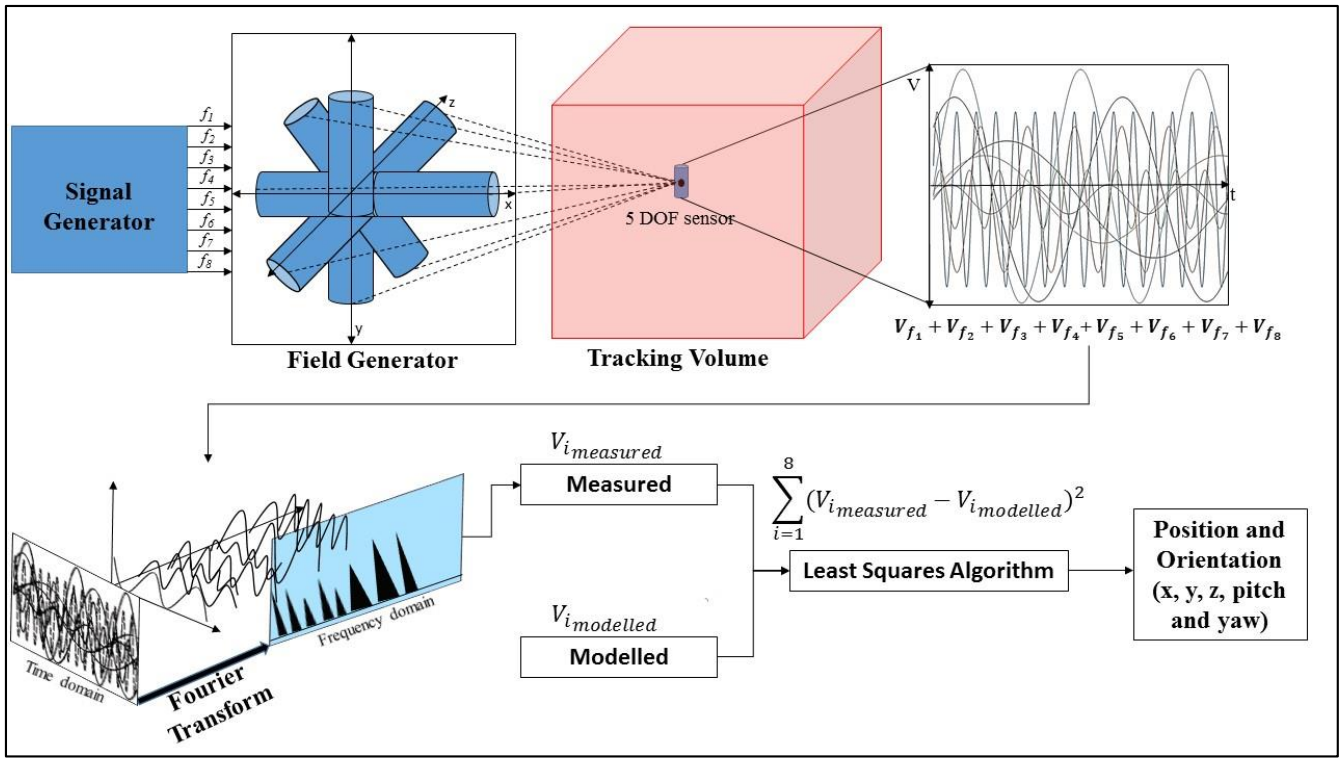

Figure 5. EMN system framework. A signal generator drives each emitter coil with a signal that has a different amplitude and frequency. In the tracking volume located above field generator a voltage is induced in a tracked 5 DOF sensor. The components of the induced voltage are then separated from one another using a fourier transform. The separated components are then used in a least squares algorithm to deterimine the position and orientation of the tracked sensor within the tracked volume with respect to the emitter coils.

1.5.3.2.1 Field generator

The FG is the electromagnetic source that houses the emitter coils [117]. Each of the emitter coils in a FG is powered by a sinusoidal current at a unique frequency. The known geometry of the magnetic fields around the FG is defined as the tracking volume [117].

1.5.3.2.2 Electromagnetic sensing coil

An electromagnetic sensing coil is composed of a helical coil of wire wound around a magnetically permeable core [92, 98]. When an electromagnetic sensing coil is located in the tracking volume of an EMN system a voltage is induced in the sensing coil. The induced voltage is a composite signal that is a result of each emitter coil in the FG inducing a voltage in the sensor [92, 120]. For it to be possible

to resolve the position and orientation of the sensor the composite induced voltage needs to be decomposed into constituent induced voltages [120]. The constituent induced voltages have different frequencies and amplitudes and are obtained by applying a Fourier transform to the periodically sampled composite signal [92]. The constituent voltages are then used in a least-squares algorithm to determine the position and orientation of the sensor [92].

1.5.3.2.3 Position and orientation determination

An accurate mathematical model of the generated magnetic fields is a necessary component in the design of an EMN system [126]. The model is a set of analytical expressions that are important for the prediction of the physical interaction between the system FG and the electromagnetic sensing coil [126]. Unknown parameters of the mathematical model for an EMN system are determined experimentally through a calibration procedure [124]. The calibration of an EMN system is performed by acquiring induced voltages of a sensing coil at known positions and orientations relative to each emitter coil [124]. This procedure experimentally refines the mathematical model of the system by providing it with scaling factors for each emitter coil [124].

The position and orientation of a sensor are determined by attempting to fit measured sensor voltages to those of the calibrated model [124]. Starting from an initial guess position and orientation an iterative non-linear least-squares optimization algorithm is used to compare the modelled voltages to the measured voltages. The position and orientation that minimizes the error for all measured and modelled voltages are calculated as the resolved sensor position and orientation [124].

1.5.3.3 Measurement uncertainty

A concern with EMN as a guidance method is that it is susceptible to distortions caused by the magnetic or electrically conductive objects situated in close proximity to the tracking volume of the system [93, 95]. When in close proximity to the tracking volume, eddy currents are induced in surrounding metallic materials due to the AC fields of the FG. The induction of eddy currents results in the disturbance of the magnetic fields produced by the FG and as a result of the distortion introduced the accuracy of the EMN system is affected [93]. In a clinical brachytherapy environment, such sources of field distortion include medical imaging devices, patient immobilization equipment

and surgical instruments [95]. Furthermore, ferromagnetic objects become strongly magnetic in the presence of an electromagnetic field, which can act as another source of field distortion for EMN [97].

1.5.3.4 Minimizing measurement uncertainty

The distortion of reference magnetic fields, as a result of the presence of ferromagnetic objects and electronic equipment, is difficult to characterize analytically [102]. The distortion in the magnetic fields causes dynamic and static errors in position measurements provided by the EMN system [102]. Depending on the clinical environment, accuracy in the EMN system's sensor readings for position may vary [102]. A method that can help minimize the amount of field distortion for current EMN systems is the optimum positioning of the patient, mobilization equipment, imaging devices, and FG within a working area [95]. By optimizing the arrangement of the working area in which an EMN system operates, positioning error can be reduced with a decreased sensor to FG distance, and moving field distorting objects further away from the FG and sensor [103]. The accuracy in measurements provided by the EMN system are dependent on isolating potential sources of field distortion from the volume of interest [103].

1.5 Research problem

1.6.1 Definition of research problem

There is a scarcity of definitive comparative studies in the literature involving the use of real-time guidance for the catheter placement in P-ISBT. The lack of adequate and accessible real-time guidance for catheter placement is a significant issue that contributes to the difficulty associated with the P-ISBT technique for gynecological cancers [28, 87, 90]. In addition to minimizing the difficulty associated with the technically challenging nature of P-ISBT, real-time guidance during the implant procedure has demonstrated improvements in implant geometry [87]. Optimal implant geometry is associated with uniform dose across the target volume and minimized dose to OARs while poor quality implants are linked to less desirable patient outcomes [34, 91]. A proposed solution to address the national and global concerns for an adequate, accessible, and low resource real-time guidance method is an electromagnetic navigation system.

1.6.2 Hypothesis

The use of electromagnetic navigation as a guidance system during P-ISBT implant procedures will improve implant geometry, specifically catheter straightness and spacing.

1.6.3 Primary objective

The primary objective of this study is to compare implant quality when using electromagnetic navigation in comparison to when using the standard clinical workflow. The implant quality is defined by decreased catheter deflection and uniform catheter spacing in an implant.

1.6.4 Secondary objectives

The secondary objective of this study is to assess the difference in time when using electromagnetic navigation in comparison to when using the standard clinical workflow for the P-ISBT process.

Chapter 2 Validation and clinical application of an electromagnetic navigation system

2.1 Abstract

Purpose

Perineal-based interstitial brachytherapy (P-ISBT) is an essential component of the therapeutic management for gynecological cancers. By incorporating electromagnetic navigation into the P-ISBT implant procedure, implant quality may be improved. The goal of this work is to quantify the impact electromagnetic navigation (EMN) has on implant quality, with the overall intent of enabling improved treatment outcomes for gynecological cancer patients undergoing P-ISBT.

Materials and Methods

An EMN system was developed in-house at the Odette Cancer Centre. The tracking accuracy and precision of the system were characterized using a machined phantom. Following a pre-clinical validation, the EMN system was used in the first of two P-ISBT implant procedures for 5 gynecological cancer patients as part of an ongoing prospective clinical trial. The second of the two implant procedures were performed using the standard clinical workflow (SCW). Using the data obtained from both implant procedures for each patient, an interpatient and intrapatient analysis was conducted where the EMN implants were compared to the SCW implants. The catheters paths in each implant procedure were exported from the Oncentra Brachy treatment planning software (Elekta AB, Sweden) and analyzed using MATLAB. Implant quality was evaluated by using the exported positional data to determine catheter deflection and catheter spacing.

Results

The phantom-based validation of the EMN system in a distortion-free environment and a gynecological brachytherapy operating room (OR) environment yielded operational system accuracy of < 0.1 mm and jitter of < 1.00 mm in both environments. Clinical trial results indicated that the mean and standard deviation of catheter deflection reported when EMN was used for catheter placement was 3.52 +/- 2.53 mm compared to 5.48 +/- 3.63 mm when the standard clinical workflow was used. Also, the mean and standard deviation of catheter spacing noted when using EMN was 9.31 +/- 4.81 mm compared to 7.09 +/- 6.06 mm when the SCW was followed. Catheter deflection and catheter spacing were noted to significantly improve when EMN was used in comparison to when the SCW was used.

Conclusions

The results of this study demonstrate that electromagnetic navigated catheter placement is promising

as a real-time guidance option in the P-ISBT workflow for gynecological cancers.

2.2 Introduction

For gynecological malignancies that are large or complex asymmetric tumours with/without vaginal involvement, perineal-based interstitial applicators are indicated [73]. The addition of the interstitial technique involves the insertion of catheters into the tumour enabling a higher dose conformity and normal tissue sparing. The addition of interstitial catheters is linked to improvements in local control for tumours larger than 30 cm^3 [73]. It has been demonstrated that at least 70% of gynecological brachytherapy cases can benefit from interstitial catheters [28]. Although there are benefits with interstitial application, adoption of this technique is limited.

The lagging adoption of perineal-based interstitial brachytherapy (P-ISBT) for gynecological malignancies is primarily due to the lack of expertise with insterstitial techniques. Real-time guidance during the insertion of catheters has been demonstrated to reduce the reliance on expertise and improve the accesibilty of the technique, as it has been found with interstitial prostate brachytherapy [28]. The lack of real-time guidance is a cause for concern that has been linked with implant quality uncertainty [131]. Optimal catheter positioning, which is reflective of implant quality, is indirectly associated with the potential for optimal treatment delivery [134]. To address the uncertainty associated with implant quality, electromagnetic navigation (EMN) is a potential real-time guidance option that can be used in the P-ISBT workflow. By incorporating EMN into the current workflow it may be possible to achieve improved implant quality [38].

This study reports the results of a two-part evaluation of a custom built EMN system dedicated for use in the gynecological P-ISBT workflow. The first characterizes the tracking accuracy and jitter of the system. The second part presents interim results from an ongoing prospective clinical trial that aims to evaluate implant quality when using EMN as part of the P-ISBT workflow in comparison to implant quality when the standard clinical workflow (SCW) is followed.

2.3 Methods and materials

2.3.1 Electromagnetic navigation system

The navigation consists of an Aurora V3 Planar Field Generator (North Digital Inc., Waterloo,

Canada), 5 DOF sensors (North Digital Inc., Waterloo, Canada), 6 DOF sensors (North Digital Inc., Waterloo, Canada), and a computer system to provide visual feedback. The 5 DOF sensor is housed in a stainless steel stylet that can fit in 6 F plastic proguide needles (Elekta AB, Sweden). The 6 DOF sensor is housed in a removable insert that attaches to the vaginal cylinder and tracks its position. The EMN system is shown in *Figure 6*. The field generator and sensors are electronic components that were acquired and integrated to an in-house built EMN navigation system, which consisted of surgical tool bodies and software that was developed at the Odette Cancer Centre.

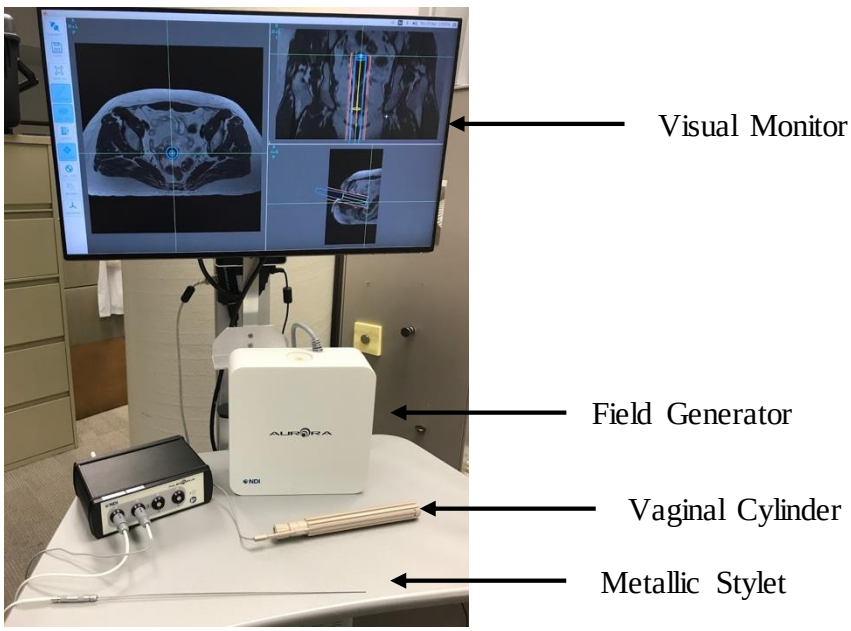

Figure 6. EMN system components.

A user interface was designed in Python 3.5 to provide real-time feedback for the catheter position overlayed on the pre-brachytheapy MR imaging.

The 5 DOF sensor was integrated into a stainless-steel stylet that was 294 mm in length and 1.47 mm in diameter. The stylet is shown in *Figure 7*. The sensor was fixed within the tool body so that the sensor's tip was flush with the stylet's tip. The 5 DOF sensor reports the position and orientation as translations in the *x*, *y* and *z* axes, and rotations around the *x* and *y* axes. Rotation around the *z*-axis for the 5 DOF sensor is not provided and this is the primary difference between the 5 DOF and 6 DOF sensor.

Figure 7. 5 DOF tracked metallic stylet.

The 6 DOF sensor was incorporated into a vaginal cylinder as a removable insert as shown in *Figure 8*. The vaginal cylinder measured 22 mm in diameter and was composed of polyether ketone plastic. The 6 DOF sensor reports the position and orientation as translations in the *x*, *y* and *z* axes, and rotations around the *x*, *y* and *z* axes. By reporting the rotation in the z-axis for the tracked cylinder it is possible to determine if the cylinder has been inserted in the same orientation that it was planned for.

Figure 8. Disassembled 6 DOF tracked vaginal cylinder.

2.3.2 Pre-clinical validation

Before using the EMN system clinically, tracking accuracy and jitter of the system was characterized through phantom-based validation.

Phantom design

The phantom pictured in *Figure 9* was constructed using two parallel acrylic plates. Both plates contained a grid pattern of 48 holes that resembled the Syed-Neblett template grid used in the P-ISBT implant procedure. In the centre of the both plates, a 22 mm opening was created to fit the vaginal cylinder. Hollow delrin tubes that were custom sized for the tracked metallic stylet were inserted through each of the grid positions and then epoxied to both plates. The geometry of grid positions in the phantom served as the ground-truth values when characterizing the tracking accuracy and precision of the EMN system.

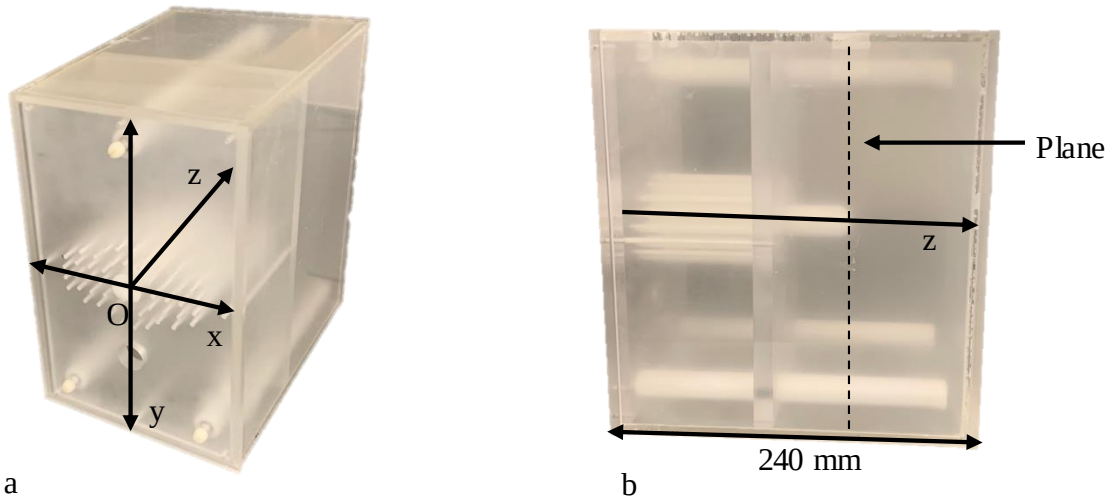

Figure 9. (a) Gynecological P-ISBT phantom. O is the user-defined origin that is located at the center of the phantom surface plate. A 3-D sweep of EMN measurements was performed by inserting the tracked metallic stylet into each of the 48 delrin tubes. (b) Side view of phantom. The dotted line represents an example of a plane in which measurements were taken in.

Phantom-based validation

The field generator (FG) produces a magnetic field that is used to locate tracked tools. The EMN system measures and reports the position of the tracked metallic stylet with respect to the tip of the tracked vaginal cylinder, through a series of coordinate transformations. The CAD design of the phantom was used as the ground truth to comprehensively test the positional tracking accuracy of the EMN system. *Figure 9*, indicates the position of the origin at center of the phantom surface plate. Each of the tubes in the phantom run parallel to each other and are equally spaced 10 mm apart. Positional data was acquired by inserting the tracked metallic stylet of the EMN system into each of the delrin tubes. The positional data was acquired for each hole position on the template face for 4 planes along the z-axis of the phantom (refer to *Figure 9*). At each spatial location, 200 measurement samples at 40 Hz were obtained using the EMN system [42]. The 3-D sweep was performed in a controlled laboratory environment and a gynecological brachytherapy operating room (OR) environment. The accuracy and jitter of the measurements for both environments were used to evaluate the impact of clinical equipment that may distort the magnetic field. Each measurement session was conducted three times for each environment over a course of three days to ensure reproducibility.

Accuracy

The tracking accuracy of the system was reported as the mean error in the *x*, *y*, and *z* directions

between the EMN system reported coordinates and phantom coordinates.

Jitter

The averaged jitter was a measure of the fluctuation of repeated EMN system measurements at fixed spatial locations within the phantom. The jitter was computed as the root mean square error (RMSE) in the *x*, *y*, and *z* direction.

Experimental setup

The experiments were performed both in a controlled laboratory environment (*Figure 10a*) and in a gynecological brachytherapy OR environment (*Figure 10b*) [42]. A survey of the controlled laboratory environment was performed using a magnetometer to confirm anomalies were not present in the measurement area. In addition to surveying the area, to ensure it was a ferromagnetically clean environment, the FG was positioned at least 50 cm away from any potentially distorting equipment. The OR tests were conducted to evaluate the potential impact of the presence of clinical equipment around the tracked volume [42]. To replicate a potentially distorting environment, a typical gynecological brachytherapy procedural setup was recreated that included an operating room table, leg stirrups, a foot stool and a surgical cart (*Figure 10b*) [42]. The tracking accuracy and jitter achieved in the OR configuration represented the lower limit of the performance of the system [42].

Figure 10. (a) Clean room. (b) Gynecological brachytherapy OR environment

2.3.3 Patient study

From May 2019 to Febuary 2020, 5 women diagnosed with gynecological malignancies were enrolled in an ongoing trial at the Odette Cancer Centre. As per the standard of care, the enlisted patients received MRI-based high-dose-rate P-ISBT treatment using an intracavitary vaginal applicator and a Syed-Neblett template [127]. A total of two implant procedures, spaced a week apart were performed for each patient. Patients were accrued as part of a research ethics board approved clinical trial. The EMN system was used to guide catheters for the first implant procedure in each of the patients. The second implant procedure occurred following the SCW. The positional data of the catheter trajectories was exported from the treatment planning software, Oncentra Brachy (Elekta AB, Sweden) and analyzed using MATLAB. The purpose of the patient study was to evaluate the clinical impact an EMN system has on the P-ISBT workflow by comparing the implant quality for the first implant procedure when EMN was used in comparison to the second implant procedure using the SCW.

Standard clinical workflow

Four fractions of brachytherapy are delivered for each patient. A week prior to the first fraction a pre-brachytherapy 3D T2-weighted MR image was acquired with an isotropic resolution of 1mm. Images were acquired with a vaginal cylinder in place to act as a fiducial for subsequent registration and aid in planning the implantation. The purpose of this image was to determine the geometry of the treatment volume and to assist in preplanning for the catheter placement. The first implant procedure was used to deliver the first and second fraction. After the first fraction was delivered the second fraction was delivered the following morning. The second implant procedure was used to deliver the third and fourth fraction. Similarly, the third fraction was delivered and then the following morning the fourth fraction was delivered. Each implant procedure was spaced a week apart. Prior to treatment delivery for each fraction an MR image was taken to plan the treatment for the patient. Planning consists of contouring the targets and organs at risk on the MR images, while simultaneously identifying the implanted catheters and applicators. The plan is then generated by using a hybrid inverse planning and optimization algorithm termed HIPO [137]. This inverse planning algorithm optimizes the dose based on the targets, organs at risk and the catheter arrangement at the time the image was taken. The standard clinical workflow was used to place catheters for the second implant procedure to deliver the third and fourth fraction. Both the SCW

and EMN workflow were identical in the pre-brachytherapy MRI assessment, the treatment planning and the treatment delivery. The primary difference in the EMN workflow is the use of EMN during first implant procedure to place catheters in real-time using spatial tracking in addition to the standard preoperative preplanning information available from the pre-brachytherapy MR image.

EMN clinical workflow

The pre-brachytherapy MR image was imported into the EMN system software prior to the first implant procedure. The software contains a library that contains a CAD model of the vaginal cylinder used in the P-ISBT implant procedure. The CAD model of the vaginal cylinder also incorporates the position of the 6 DOF EM sensor embedded in the vaginal cylinder that is tracked using the EMN system during the implantation procedure. Using the registration module in the software, the CAD model is interactively aligned with the vaginal cylinder visible in the pre-brachytherapy MRI. Once aligned, a rigid transfomartion was exported for use at the time of the implant procedure. This registration step correlates the pre-brachy MR imaging with the tracked cylinder at the time of the implant and establishes the general coordinate system. During the catheter implantation procedure the vaginal cylinder was tracked in real-time and the positions of the catheters relative to the cylinder were superimposed on the MR images. The T2-weighted images were used to display the target volume and direct the catheters during the insertion procedure. While the relative position of the catheters to the soft-tissue anatomy may be different from the time of pre-brachy imaging, the relative position of the catheters to the vaginal cylinder are based on a rigid coordinate system and are accurately represented using EMN. As such, this technique can be used to ensure a good quality implant, which is parallel and uniformly dispersed.

Registration of EMN data and Pre-brachytherapy MRI

The rigid registration of EMN data and the pre-brachytherapy MRI was achieved by using the vaginal cylinder as a fiducial marker. Intra-operatively, a series of rigid body transformations were applied to transform tracking data from the stylet and imaging data to the coordinate system of the tracked vaginal cylinder [42]. *Figure 11* represents the transformations used to align the tracked stylet to the pre-brachytherapy MR image. The pre-brachytherapy images are imported into the EMN system. In the EMN software, a purple colored CAD model of the vaginal cylinder is

overlayed onto the MR image. Then the CAD model is interactively aligned with the vaginal cylinder in the MR image. Once alignment is completed the MR image is in the frame of the CAD model, $T_{MRI \rightarrow Model}$, which is exported and used at the time of the implant procedure. During the implantation procedure guided by EMN, the tracked cylinder is first positioned so that it abuts the top of the vagina with an attempt to replicate the geometry achieved during pre-brachytherapy imaging. The CAD model of cylinder in the EMN system also captures the position of the the tracked sensor housed within the cylinder, $T_{Model \rightarrow Ref}$, is applied in the backend of the software to attain the CAD model with respect to the tracked reference cylinder. After having applied these transformations, the MR image displayed on the navigation screen is in the frame of the tracked cylinder. The position and orientation of the tracked reference cylinder and tracked metallic stylet are reported with respect to the origin of the field generator. Therefore, the following transformations are required to relate the stylet position to the reference frame of the cylinder, $(T_{Ref \rightarrow FG})^{-1} \cdot T_{Stylet \rightarrow FG}$.

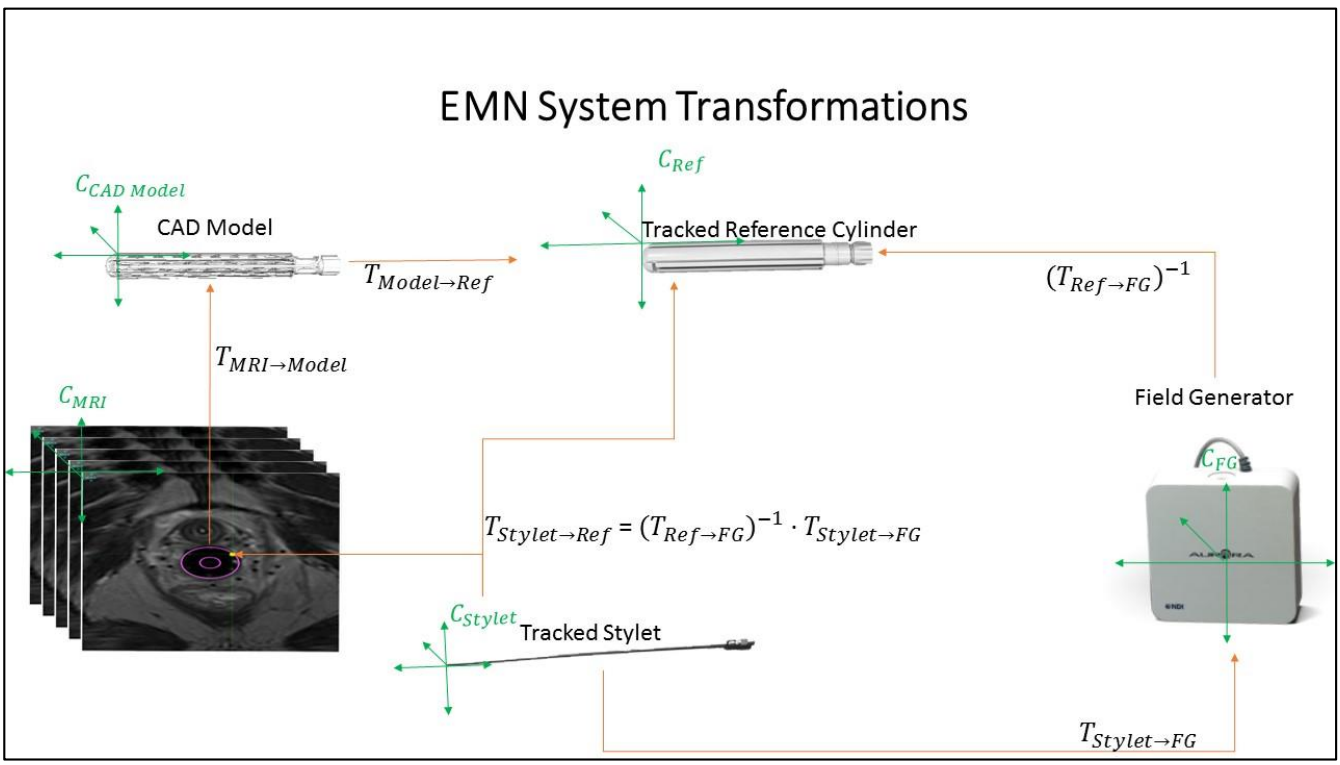

Figure 11. EMN transformations applied at the time of the first implant procedure to track catheters in real-time with respect to the tracked vaginal cylinder. The tracked catheters are *visualized in the pre-brachytherapy MRI simultaneously.*

Catheter deflection

The catheters paths for the implants under examination was acquired from Oncentra Brachy (Elekta AB, Sweden) and analyzed using MATLAB software [40]. The metric used to quantify the catheter deflection was the Hausdorff distance (HD) [106]. The HD represented the maximal difference between an ideal catheter trajectory and the actual implanted catheter trajectories. The ideal catheter geometries were represented as parallel catheter trajectories from the template parallel to the longitudinal axis of the vaginal cylinder. The region of interest for catheter deflection was isolated to the high-risk clinical target volume (CTV_{HR}). Catheters within a 10 mm margin around the CTV_{HR} were included.

Catheter spacing

The same region of interest, the CTV_{HR} with an additional 10 mm margin, was used for catheter spacing. The metric used to quantify the spacing of catheters was the Euclidean distance. A *k*-nearest neighbour search was performed for each slice of the CTV_{HR} to determine the spacing of adjacent catheter trajectories that were used for treatment.

Time

A secondary quantitative metric for the study was the recorded operative time in minutes for the implant procedure when EMN was used in comparison to when the SCW was followed. The start time that was recorded indicated when the patient was placed under anesthesia and the stop time was recorded as the time when the radiation oncologist finished the interstitial catheter implantation procedure. This metric was recorded to capture the impact of implementing the EMN system on the operating room flow and efficiency.

2.4 Results

2.4.1 Preclinical validation

Accuracy

Figure 12 represents the positional error recorded for the *x*, *y* and *z* direction when using the EMN system. The mean error in the *x*, *y* and *z* direction in the clean room environment was 0.01 mm, -0.02 mm and 0.01 mm, respectively. The performance of the EMN system in the brachytherapy operating room environment was comparable with -0.03 mm, 0.03 mm, and 0.08 mm errors in the *x*, *y*, and *z* direction noted, respectively. There was no statistically significant difference in the tracking errors between the two environments ($p>0.05$).

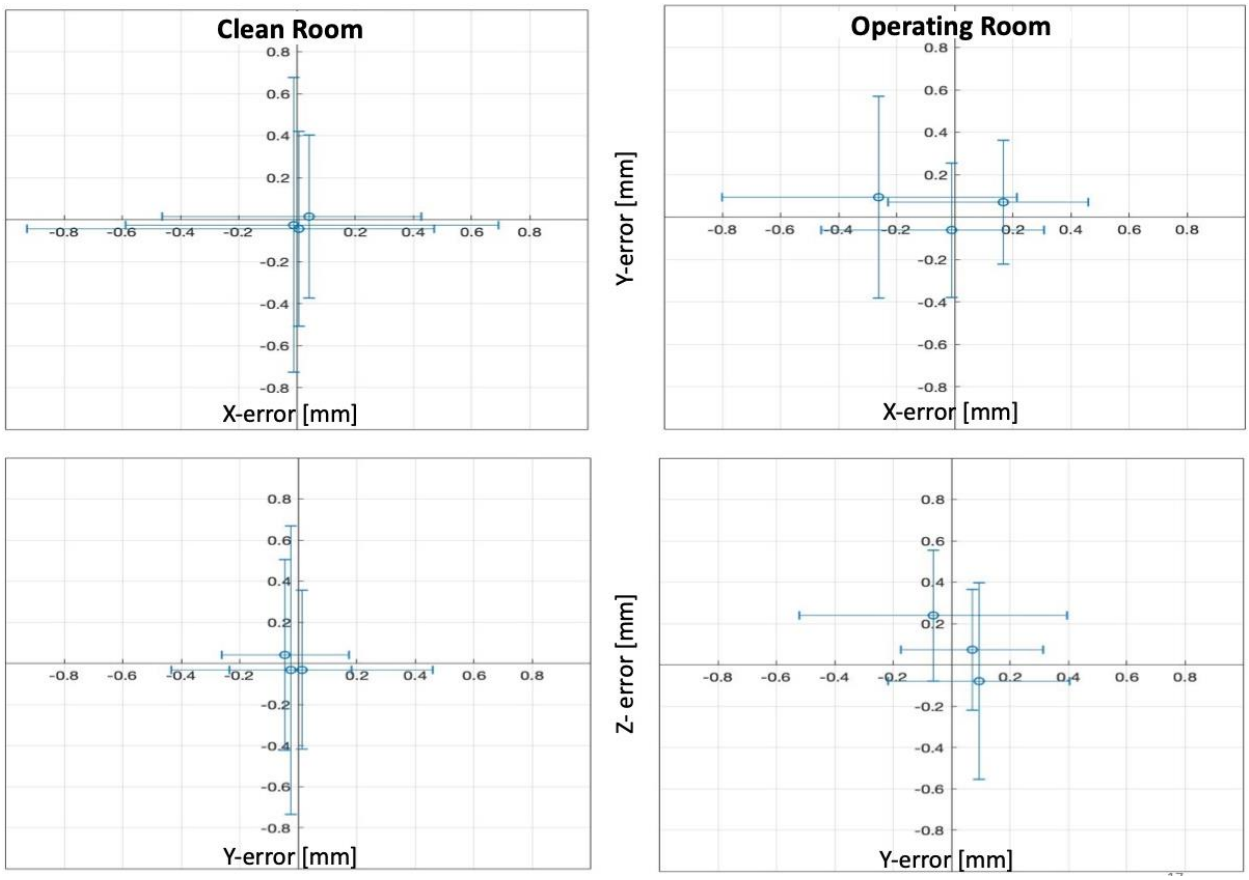

Figure 12. Visual representation of averaged positional error in the x, y and z direction for EMN system measurements taken in the clean room environment versus the gynecological brachytherapy OR environment. The error bars represent the standard deviation.

Jitter

Table 2 presents the jitter for EMN system-generated measurements in the cleanroom and operating room environment. The average jitter measured in the *x*, *y* and *z* direction in the clean room was 0.49 mm, 0.37 mm and 0.36 mm, respectively. The average jitter in the operating room measured in the x-, y-, and z-direction was 0.70 mm, 0.53 mm and 0.31 mm. The characterization of jitter in both environments did not indicate that there is any statistically significant difference between the two ($p>0.05$).

Table 2. Jitter calculations in the x, y and z direction for EMN system generated measurements using the P-ISBT phantom-based validation method. The combined mean and standard deviation are displayed for each direction, with the mean preceding the standard deviation.

Direction	Clean Room	Operating Room
x [mm]	0.49 +/- 0.09	0.70 +/- 0.23
y [mm]	0.37 +/- 0.10	0.53 +/- 0.16
z [mm]	0.36 +/- 0.13	0.31 +/- 0.15

2.4.2 Patient Study

Catheter Deflection

Figure 13 shows a 3D rendering of catheter paths from the EMN guided implant, displayed in the left panel, and the implant that was performed using the SCW, displayed in the right panel. The turquoise trajectories in *Figure 12* depict the catheter geometry. The red positions in the image represent the active dwell positions along the catheter that were used for treatment delivery. From the catheter trajectories seen in *Figure 12*, a significantly deflected catheter is visible in the SCW implant.

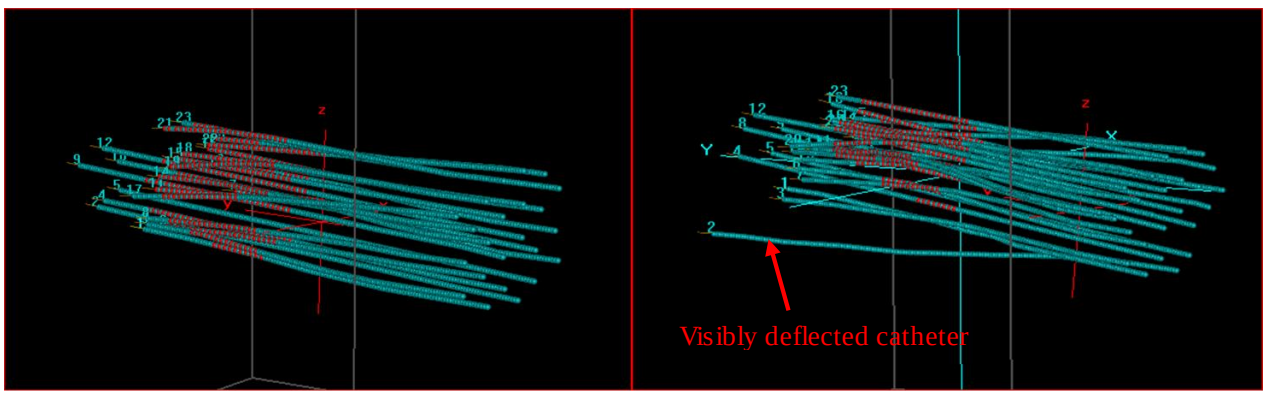

Figure 13. An example of the impact that the addition of EMN can have on the placement of catheters during the P-ISBT implant procedure.

Figures 14 and *Figure 15* illustrate catheter deflection per patient and as an average over all patients following the P-ISBT implant procedure, respectively. *Figure 13* reports the catheter deflection measured for each implant procedure performed for the 5 patients that were enlisted in the clinical trial. The analysis of catheter deflection was confined to the catheters that were within a

10 mm margin around the $CTV_{HR.}$ There were statistically significant reductions in catheter deflection for the EMN implant procedure for each patient in comparison to the SCW implant procedure ($p<0.05$).

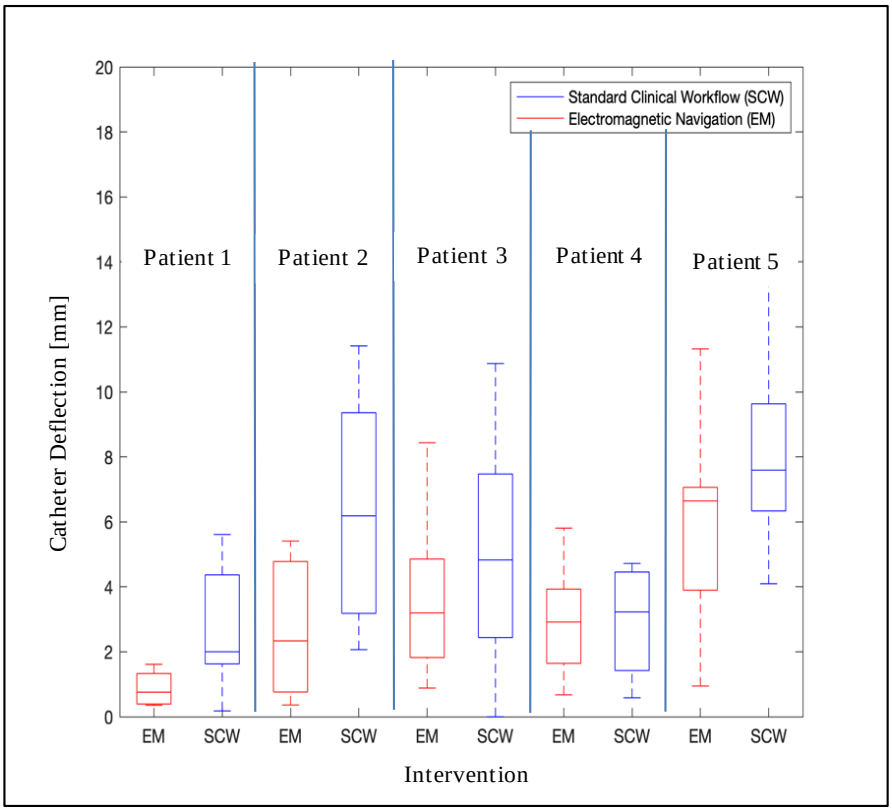

Figure 14. Catheter deflection that was reported on a per patient basis for the 5 patients enrolled in the clinical trial.

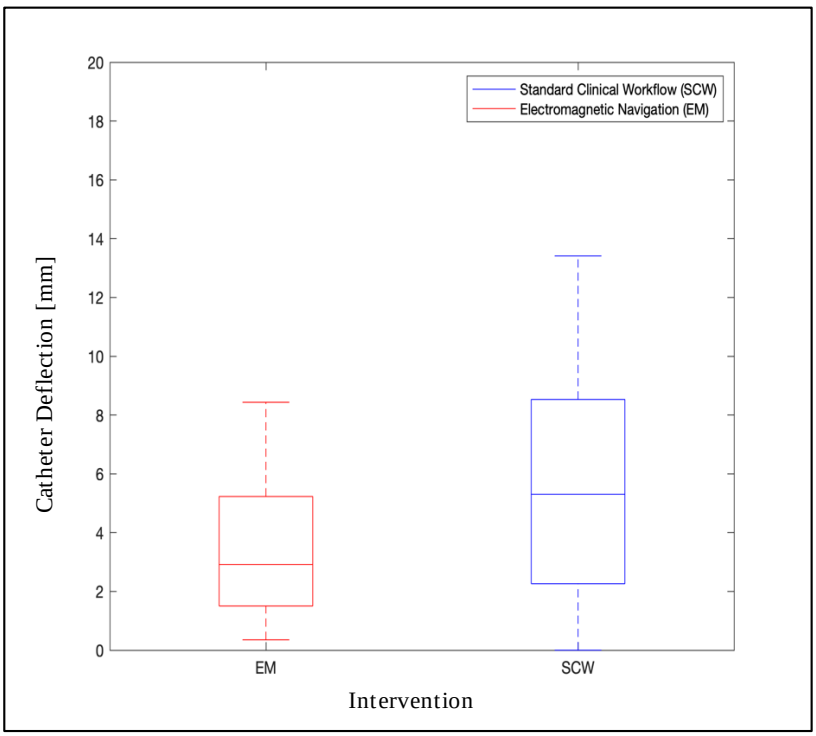

Figure 15. The data represents the overall catheter deflection, where the first implant procedure and second implant procedure for all patients were grouped together under the EM and SCW group, respectively.

Catheter Spacing

Figure 16 and *Figure 17* represent catheter spacing within the CTV_{HR} volume for the EMN and SCW group for a total of five patients. The nearest neighbour distances was aggregated and plotted as a histogram. Ideal catheter spacing is 10 mm when using the Syed-Neblett template, the boxplot graphically represents an approximation of how close the achieved catheter spacing is to its ideal configuration.

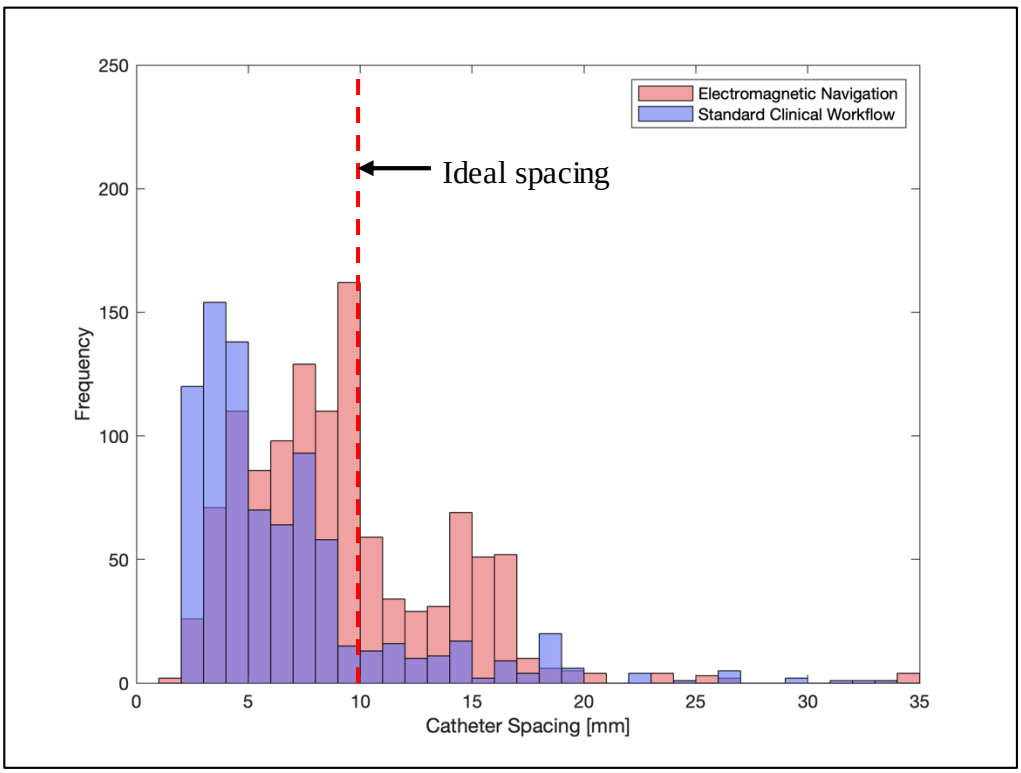

Figure 16. A visual representation of catheter spacing in the CTV_{HR} volume for implant procedures performed using EMN and SCW.

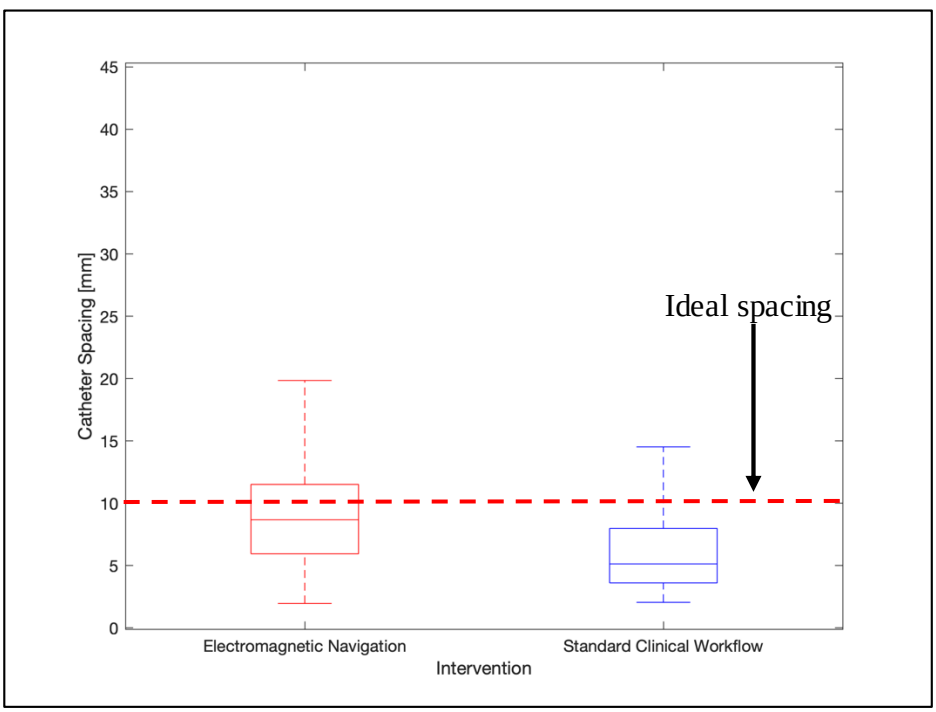

Figure 17. The data represents the overall catheter spacing where the line in the box represents the median and the lower and upper edges of the box represent the 25th and 75th percentile, respectively.

Implant quality

Table 4 summarizes the overall implant quality and intraoperative time when P-ISBT implants were performed using EMN in comparison to when the SCW was used. A statistically significant reduction in catheter deflection and statistically significant improvement in catheter spacing was noted in the EMN group in comparison to the SCW group ($p<<0.05$). An improvement in overall implant quality was associated with the use of EMN during the P-ISBT implant procedure. The table also summarizes the average time it takes to perform an implant when using EMN in comparison to using SCW. The difference in time for the EMN group and the SCW group was not statistically significant ($p>0.05$).

Table 3. Overall implant quality comparison between the EMN group and the SCW group

		Electromagnetic Navigation	**Standard Clinical Workflow**	**P-value**
Catheter Deflection [mm]	Mean	3.52 +/- 2.53	5.48 +/- 3.63	$p << 0.05$
Catheter Spacing [mm]	Mean	9.31 +/- 4.81	7.09 +/- 6.06	$p << 0.05$
Implant time [min]	Mean	50.00 +/- 18.80	38.20 +/- 15.29	$p > 0.05$

2.5 Discussion

Validation of the EMN system in a gynecological brachytherapy OR environment achieved submillimeter operational system accuracy and jitter. In addition, there was no significant difference between when EMN system measurements were performed in a distortion-free environment compared to when they were performed in the gynecological brachytherapy OR environment. The results presented in the pre-clinical validation provided early evidence supporting subsequent testing of the EMN system as part of a clinical study. The catheter deflection reported during the trial was 3.52 +/- 2.53 mm and 5.48 +/- 3.63 mm when using the EMN system and the SCW, respectively. Minimal catheter deflection as noted in the EMN arm is ideal since it helps evenly distribute active dwells throughout the CTV_{HR}, which will help modulate dose and improve coverage and conformality. Similar to the improvement observed in catheter deflection, the catheter spacing documented in the trial was 9.31 +/- 4.81 mm and 7.09 +/- 6.06 mm when using the EMN system in comparison to the SCW, respectively. As a result of the statistically significant improvements in both parameters, improvement in implant quality were noted when EMN was used during the implant procedure. Another metric examined during the trial was the time. Although the difference in intraoperative time was not statistically significant, the average time it took to perform an implant was longer, 50 minutes, when EMN was used in comparison to, 38 min, when using the SCW. The results from this work demonstrate that electromagnetic navigated catheter placement is promising, and clinically feasible as a real-time guidance option in the P-ISBT workflow for gynecological malignancies.

Prior work by Zhou *et al.* evaluated EMN system performance in an OR environment. This work reported that a tracking accuracy of 1.6 +/- 0.2 mm was achievable in a high distortion environment. The OR configuration used in this study simulated a typical prostate brachytherapy procedural set-up [127]. The surrounding equipment in the set-up included an ultrasound machine, a treatment planning computer console, stirrups, a stepper unit, an ultrasound probe, and a C-arm imaging system [127]. The stepper unit and ultrasound probe were located within the field of view of the tracking system. In addition to the existing interference, additional distortion was present due to the FG being positioned underneath the mechanical treatment bed. In similar studies conducted by Boutaleb *et al.*, and Franz *et al.* tracking accuracy of 1.5 - 2 mm was achieved in high distortion environments resembling variations of the prostate brachytherapy configuration [53, 129]. For each

of the studies mentioned above, submillimeter accuracy and jitter was achieved when the EMN system performance was characterized in a low distortion environment [127]. The distinct difference for low-distortion environments in these studies was the removal of distorting equipment from the field of view of the tracking system. Therefore, low distortion environments in these studies were not identical but similar to the gynecological brachytherapy OR environment recreated in our study. The findings from the literature correlate with the results that were found in the EMN system validation presented in our study.

Although there were similar pre-clinical studies to our validation study, this is the first clinical trial to incorporate an EMN system dedicated for real-time catheter placement in P-ISBT for gynecological cancers. Interstital breast brachytherapy is the only other site to incorporate EMN into the clinical workflow for a patient trial [134, 135, 136]. As opposed to real-time guidance, each of these interstitial breast brachytherapy trials used EMN as a quality assurance tool to assess implant geometry variability after implantation. Therefore regardless of the treatment site, this study is still the first of its kind to examine the use of EMN for real-time catheter placement in brachytherapy patients.

The results from this clinical trial demonstrate favourable improvements in implant quality through the use of EMN. Although implant quality is associated with the potential for improving treatment outcomes, the relationship between implant quality and treatment outcomes is not well established. A present limitation of this study is that an unbiased dosimetric comparison between an EMN and SCW workflow was not possible. This is primarily due to the fact that image-guided adaptive brachytherapy is performed as the standard of care approach at the Odette Cancer Centre. Therefore, at each fraction, given that the target volume shrinks with each administration of brachytherapy, there is significant variability associated with treatment volumes between each implant procedure so a reliable evaluation of EMN on dosimetry was not possible.

2.6 Conclusion

In this work, a novel electromagnetic navigation system was developed to provide real-time guidance for interstitial gynecological brachytherapy. Following development, comprehensive phantom-based validation was performed to characterize the accuracy and precision of the system in a clinical environment. A clinical trial of the system demonstrated that EMN improves implant

quality by decreasing catheter deflection and improving catheter spacing. Based on the results of the present study there is potential that EMN could improve treatment outcomes for P-ISBT procedures when used for gynecological cancers.

2.7 Acknowledgement

This research was funded through donations from the Allan Tiffin fund.

Chapter 3 Conclusion

3.1 Thesis overview

The focus of the thesis was to validate an EMN system and then to evaluate its impact on the P-ISBT implant procedure for gynecological cancers. In the context of this thesis, for the example of temporary implants, catheter geometry is indicated as the catheter position inside the patient in relation to target and OAR structures [110]. The placement of a sufficient number of catheters at desired locations is required for optimal dose distribution and favourable clinical outcome [87]. The lack of real-time guidance for catheter placement is a concern associated with uncertainty in optimal dose delivery [28, 87, 111]. To address the lack of real-time guidance for catheter placement during the implant procedure, EMN was proposed as a solution.

Chapter 2 described the novel EMN system, EMN system validation and results from a clinical trial where the EMN system was used during the implant procedure for catheter placement.
The hypothesis of this thesis was confirmed as it was found in the clinical trial that the use of EMN during the implant procedure improves implant quality by significantly minimizing catheter deflection and significantly improving catheter spacing. Due to the association between implant geometry and accurate dose delivery, use of EMN could potentially improve treatment outcomes for P-ISBT procedures.

3.2 Future work

Use of EMN during the implant procedure for P-ISBT was evaluated as a part of this thesis and it was found to be suitable for real-time guidance. However, there may be potential to further identify how use of EMN guidance impacts the dosimetry of implants. If EMN guidance were to show improved implant dosimetry, which is linked to better treatment outcomes, it would further solidify the need of EMN as a real-time guidance strategy. Also, although the implant quality for this subset of patients has shown to improve with the use of EMN, there is still a need to collect more data from a larger set of patients to make a clear distinction that EMN guidance results in the improvement of implant quality for gynecological cancer patients undergoing P-ISBT.

Bibliography

[1] Canadian Cancer Statistics Advisory Committee. Canadian Cancer Statistics 2018. Toronto, ON: Canadian Cancer Society; 2018. Available at: cancer.ca/Canadian-Cancer-Statistics-2018-EN (August 20, 2019). 2018 resources

[2] Forte T, Lockwood GA, McLachlin CM, et al. 2012. A first look at participation rates in cervical cancer screening programs in Canada. Curr Oncol; 19(5)

[3] Kim J, Bell C, Sun M, et al. 2016. Effect of human papillomavirus vaccination on cervical cancer screening in Alberta. CMAJ; 188(12): E281-8

[4] Hariri S, Bennett NM, Niccolai LM, et al. 2015. Reduction in HPV 16/18-associated high grade cervical lesions following HPV vaccination introduction in the United States-2008-2012. Vaccine; 33(13): 1608-13

[5] Ferlay J, Soerjomataram I, Ervik M, et al. GLOBOCAN 2012 v1.0, Cancer incidence and mortality worldwide: IARC CancerBase No. 11. Lyon, France

[6] Louchini R, Beaupré M. Cancer incidence and mortality among Aboriginal people living on reserves and northern villages in Quebec, 1988–2004. Int J Circumpolar Health2008;67:445–451

[7] GLOBOCAN Cancer Fact Sheets: Cervical cancer. (n.d.). Retrieved July 19, 2019, from http://globocan.iarc.fr/old/FactSheets/cancers/cervix-new.asp

[8] Sturdza, A., Pötter, R., Fokdal, L. U., Haie-Meder, C., Tan, L. T., Mazeron, R., ... & Gillham, C. (2016). Image guided brachytherapy in locally advanced cervical cancer: improved pelvic control and survival in RetroEMBRACE, a multicenter cohort study. Radiotherapy and Oncology, 120(3), 428-433.

[9] Kay J. Park and Robert A. Soslow (2009) Current Concepts in Cervical Pathology. Archives of Pathology & Laboratory Medicine: May 2009, Vol. 133, No. 5, pp. 729-738.

[10] Takeuchi S. (2016). Biology and treatment of cervical adenocarcinoma. Chinese journal of cancer research. Chung-kuo yen cheng yen chiu, 28(2), 254–262. doi:10.21147/j.issn.1000-9604.2016.02.11

[11] Chengxia Zheng, Song Qing, Jing Wang, Guodong Lü, Hongyi Li, Xiaoyi Lü, Cailing Ma, Jun Tang, Xiaxia Yue, Diagnosis of cervical squamous cell carcinoma and cervical adenocarcinoma based on Raman spectroscopy and support vector machine, Photodiagnosis and Photodynamic Therapy,Volume 27, 2019, Pages 156-161.

[12] Wright, A. A., Howitt, B. E., Myers, A. P., Dahlberg, S. E., Palescandolo, E., Van Hummelen, P., . . . Hirsch, M. S. (2013). Oncogenic mutations in cervical cancer: Genomic differences between adenocarcinomas and squamous cell carcinomas of the cervix. Cancer, 119(21), 3776-3783. doi:10.1002/cncr.28288

[13] Vizcaino, A. P., Moreno, V., Bosch, F. X., Muñoz, N., Barros-Dios, X. M., Borras, J., & Parkin, D. M. (2000). International trends in incidence of cervical cancer: II. Squamous-cell carcinoma. International Journal of Cancer, 86(3), 429-435. doi:10.1002/(SICI)1097-0215(20000501)86:3<429::AID-IJC20>3.0.CO;2-D

[14] Seamon, L. G., Java, J. J., Monk, B. J., Penson, R. T., Brown, J., Mannel, R. S., ... & Liao, S. Y. (2018). Impact of tumour histology on survival in advanced cervical carcinoma: an NRG Oncology/Gynaecologic Oncology Group Study. British journal of cancer, 118(2), 162.

[15] Green, J., Berrington de Gonzalez, A., Sweetland, S., Beral, V., Chilvers, C., Crossley, B., … Vessey, M. P. (2003). Risk factors for adenocarcinoma and squamous cell carcinoma of the cervix in women aged 20-44 years: the UK National Case-Control Study of Cervical Cancer. British journal of cancer, 89(11), 2078–2086. doi:10.1038/sj.bjc.6601296

[16] Johnson, C. A., James, D., Marzan, A., & Armaos, M. (2019, March). Cervical cancer: an overview of pathophysiology and management. In Seminars in oncology nursing. WB Saunders.

[17] Catherine Devine, Chitra Viswanathan, Silvana Faria, Leonardo Marcal, Tara L. Sagebiel, Imaging and Staging of Cervical Cancer, Seminars in Ultrasound, CT and MRI, Volume 40, Issue 4, 2019, Pages 280-286, ISSN 0887-2171, https://doi.org/10.1053/j.sult.2019.03.001.

[18] Waggoner, S. E. (2003). Cervical cancer. *The lancet*, *361*(9376), 2217-2225.

[19] Vicus, D., Sutradhar, R., Lu, Y., Elit, L., Kupets, R., Paszat, L., & Investigators of the Ontario Cancer Screening Research Network. (2014). The association between cervical cancer screening and mortality from cervical cancer: A population based case–control study. Gynecologic oncology, 133(2), 167-171.

[20] Saraiya, M., Steben, M., Watson, M., & Markowitz, L. (2013). Evolution of cervical cancer screening and prevention in United States and Canada: implications for public health practitioners and clinicians. *Preventive medicine*, *57*(5), 426-433.

[21] Fiset, S., Welch, M. L., Weiss, J., Pintilie, M., Conway, J. L., Milosevic, M., ... & Xie, J. (2019). Repeatability and reproducibility of MRI-based radiomic features in cervical cancer. *Radiotherapy and Oncology*, *135*, 107-114.

[22] Otero-García, M. M., Mesa-Álvarez, A., Nikolic, O., Blanco-Lobato, P., Basta-Nikolic, M., de Llano-Ortega, R. M., ... & Szewczyk-Bieda, M. (2019). Role of MRI in staging and follow-up of endometrial and cervical cancer: pitfalls and mimickers. *Insights into imaging*, *10*(1), 19.

[23] Tanderup, K., Pötter, R., Lindegaard, J., Kirisits, C., Juergenliemk-Schulz, I., & De Leeuw, A. (2015). Image guided intensity modulated External beam radiochemotherapy and MRI based adaptive BRAchytherapy in locally advanced CErvical cancer EMBRACE-II. *EMBRACE II Study Protocol*, *1*.

[24] Pötter, R., Tanderup, K., Kirisits, C., de Leeuw, A., Kirchheiner, K., Nout, R., … EMBRACE Collaborative Group (2018). The EMBRACE II study: The outcome and prospect of two decades of evolution within the GEC-ESTRO GYN working group and the EMBRACE studies. *Clinical and translational radiation oncology*, *9*, 48–60. doi:10.1016/j.ctro.2018.01.001.

[25] Kirisits, C., Pötter, R., Lang, S., Dimopoulos, J., Wachter-Gerstner, N., & Georg, D. (2005). Dose and volume parameters for MRI-based treatment planning in intracavitary brachytherapy for cervical cancer. *International Journal of Radiation Oncology* Biology* Physics*, *62*(3), 901-911.

[26] Mendez, L. C., Lang, P., Patel, C., D'Souza, D., Gladwish, A., D'Alimonte, L., ... & Leung, E. (2019). A prospective analysis of catheter complications for gynecological cancers treated with interstitial brachytherapy in the 3D era. *Brachytherapy*, *18*(1), 44-49.

[27] Hanania, A. N., Myers, P., Yoder, A. K., Bulut, A., Yu, Z. H., Eraj, S., ... & Anderson, M. L. (2019). Inversely and adaptively planned interstitial brachytherapy: A single implant approach. Gynecologic oncology, 152(2), 353-360.

[28] Mendez, L. C., Lang, P., Patel, C., D'Souza, D., Gladwish, A., D'Alimonte, L., ... & Leung, E. (2019). A prospective analysis of catheter complications for gynecological cancers treated with interstitial brachytherapy in the 3D era. *Brachytherapy*, *18*(1), 44-49.

[29] Mendez, L. C., Choi, S., D'Alimonte, L., Barnes, E., Barbera, L., & Leung, E. (2017). Opioid consumption and pain in gynecological cancer patients treated with interstitial brachytherapy. Brachytherapy, 16(4), 870-876.

[30] Mendez, L. C., Weiss, Y., D'Souza, D., Ravi, A., Barbera, L., & Leung, E. (2017). Three-dimensional-guided perineal-based interstitial brachytherapy in cervical cancer: a systematic review of technique, local control and toxicities. Radiotherapy and Oncology, 123(2), 312-318.

[31] Gladwish, A., Ravi, A., Barbera, L., Mendez, L., Davidson, M., D'Alimonte, L., ... & Leung, E. (2018). Characterizing the impact of adaptive planning on image-guided perineal interstitial brachytherapy for gynecologic malignancies. Brachytherapy, 17(2), 352-359.

[32] Petric, P., & Kirisits, C. (2016). Potential role of TRAns Cervical Endosonography (TRACE) in brachytherapy of cervical cancer: proof of concept. Journal of contemporary brachytherapy, 8(3), 215–220. doi:10.5114/jcb.2016.60502

[33] Taggar, A. S., Phan, T., Traptow, L., Banerjee, R., & Doll, C. M. (2017). Cervical cancer brachytherapy in Canada: a focus on interstitial brachytherapy utilization. Brachytherapy, 16(1), 161-166.

[34] Sethi, R., Kuo, Y. C., Edraki, B., Lerner, D., Paik, D., & Bice, W. (2018). Real-time Doppler ultrasound to identify vessels and guide needle placement for gynecologic interstitial brachytherapy. Brachytherapy, 17(5), 742-746.

[35] Viswanathan, A. N., Szymonifka, J., Tempany-Afdhal, C. M., O'Farrell, D. A., & Cormack, R. A. (2013). A prospective trial of real-time magnetic resonance–guided catheter placement in interstitial gynecologic brachytherapy. *Brachytherapy*, *12*(3), 240-247.

[36] Lee, L. J., Damato, A. L., & Viswanathan, A. N. (2013). Clinical outcomes of high-dose-rate interstitial gynecologic brachytherapy using real-time CT guidance. Brachytherapy, 12(4), 303-310.

[37] Stock, R. G., Chan, K., Terk, M., Dewyngaert, J. K., Stone, N. N., & Dottino, P. (1997). A new technique for performing Syed-Neblett template interstitial implants for gynecologic malignancies using transrectal-ultrasound guidance. International journal of radiation oncology, biology, physics, 37(4), 819-825.

[38] Viswanathan, A. N., Cormack, R., Holloway, C. L., Tanaka, C., O'Farrell, D., Devlin, P. M., & Tempany, C. (2006). Magnetic resonance–guided interstitial therapy for vaginal recurrence of endometrial cancer. International Journal of Radiation Oncology* Biology* Physics, 66(1), 91-99.

[39] Erickson, B., Albano, K., & Gillin, M. (1996). CT-guided interstitial implantation of gynecologic malignancies. International Journal of Radiation Oncology* Biology* Physics, 36(3), 699-709.

[40] de Arcos, J., Schmidt, E. J., Wang, W., Tokuda, J., Vij, K., Seethamraju, R. T., ... & Viswanathan, A. N. (2017). Prospective clinical implementation of a novel magnetic resonance tracking device for real-time brachytherapy catheter positioning. International Journal of Radiation Oncology* Biology* Physics, 99(3), 618-626.

[41] Demanes, D. J., Friedman, J. M., Park, S. J., Steinberg, M. L., Hayes Jr, J. K., & Kamrava, M. R. (2012). Brachytherapy catheter spacing and stabilization technique. Brachytherapy, 11(5), 392-397.

[42] Bharat, S., Kung, C., Dehghan, E., Ravi, A., Venugopal, N., Bonillas, A., ... & Kruecker, J. (2014). Electromagnetic tracking for catheter reconstruction in ultrasound-guided high-dose-rate brachytherapy of the prostate. *Brachytherapy*, *13*(6), 640-650.

[43] Electromagnetic Actuation and Sensing in Medical Robotics, edited by Hongliang Ren, and Jinji Sun, Springer, 2017. ProQuest Ebook Central, http://ebookcentral.proquest.com/lib/ryerson/detail.action?docID=5211325. Created from ryerson on 2019-09-23 13:31:28.

[44] Much, J. (2008). Error classification and propagation for electromagnetic tracking. *Master's thesis, Technical University of Munich, München, Germany*.

[45] Kim, W., Song, J., & Park, F. C. (2017). Closed-form position and orientation estimation for a three-axis electromagnetic tracking system. *IEEE Transactions on Industrial Electronics*, *65*(5), 4331-4337.

[46] Hu, C., Song, S., Wang, X., Meng, M. Q. H., & Li, B. (2012). A novel positioning and orientation system based on three-axis magnetic coils. *IEEE Transactions on Magnetics*, *48*(7), 2211-2219.

[47] Kellermeier, M., Fietkau, R., Strnad, V., & Bert, C. (2018). Assessment of the implant geometry in fractionated interstitial HDR breast brachytherapy using an electromagnetic tracking system. *Brachytherapy*, *17*(1), 94-102.

[48] de Arcos, J., Schmidt, E. J., Wang, W., Tokuda, J., Vij, K., Seethamraju, R. T., ... & Viswanathan, A. N. (2017). Prospective clinical implementation of a novel magnetic resonance tracking device for real-time brachytherapy catheter positioning. *International Journal of Radiation Oncology* Biology* Physics*, *99*(3), 618-626.

[49] Tourais, A., Chang, A., Venkat, P., Lee, A., Demanes, D. J., & Park, S. J. (2019). Automatic Detection of Catheter Reconstruction Error, Misconnection, and Inter-Fractional Catheter Displacement in High-Dose-Rate Interstitial Brachytherapy: Data Analysis for an Electromagnetic Tracking System. *Brachytherapy*, *18*(3), S24.

[50] Tho, D., & Beaulieu, L. (2018). A Novel Electromagnetic-Tracked Scintillation Dosimeter for Accurate In Vivo Dosimetry in HDR Brachytherapy. *arXiv preprint arXiv:1812.09612*.

[51] Beaulieu, L., Racine, E., Han, D. Y., Vigneault, E., Hsu, I. C., & Cunha, J. A. M. (2018). Real-time electromagnetic tracking–based treatment platform for high-dose-rate prostate

brachytherapy: Clinical workflows and end-to-end validation. *Brachytherapy*, *17*(1), 103-110.

[52] Bharat, S., Kung, C., Dehghan, E., Ravi, A., Venugopal, N., Bonillas, A., ... & Kruecker, J. (2014). Electromagnetic tracking for catheter reconstruction in ultrasound-guided high-dose-rate brachytherapy of the prostate. *Brachytherapy*, *13*(6), 640-650.

[53] Boutaleb, S., Racine, E., Fillion, O., Bonillas, A., Hautvast, G., Binnekamp, D., & Beaulieu, L. (2015). Performance and suitability assessment of a real-time 3D electromagnetic needle tracking system for interstitial brachytherapy. *Journal of contemporary brachytherapy*, *7*(4), 280–289. doi:10.5114/jcb.2015.54062

[54] Mehrtash, A., Damato, A., Pernelle, G., Barber, L., Farhat, N., Viswanathan, A., … Kapur, T. (2014). EM-Navigated Catheter Placement for Gynecologic Brachytherapy: An Accuracy Study. *Proceedings of SPIE--the International Society for Optical Engineering*, *9036*, 90361F. doi:10.1117/12.2044381

[55] Arun, K. S., Huang, T. S., & Blostein, S. D. (1987). Least-squares fitting of two 3-D point sets. *IEEE Transactions on pattern analysis and machine intelligence*, (5), 698-700.

[56] Chen, X., & Egger, J. (2014). Development of an open source software module for enhanced visualization during MR-guided interstitial gynecologic brachytherapy. *SpringerPlus*, *3*(1), 167.

[57] Arbyn, M., Weiderpass, E., Bruni, L., de Sanjosé, S., Saraiya, M., Ferlay, J., & Bray, F. (2019). Estimates of incidence and mortality of cervical cancer in 2018: a worldwide analysis. *The Lancet Global Health*.

[58] Zaino RJ, Ward S, Delgado G, et al: Histopathologic predictors of the behaviour of surgically treated stage IB squamous cell carcinoma of the cervix: A Gynecologic Oncology Group study. Cancer 69:1750–1758, 1992.

[59] Goellner JR: Carcinoma of the cervix: Clinical pathologic correlation of 196 cases. Am J Clin Pathol 66:775–785, 1976.

[60] Stock RJ, Zaino R, Bundy BN, Askin FB, Woodward J, Fetter B, et al. Evaluation and comparison of histopathologic grading systems of epithelial carcinoma of the uterine cervix: Gynecologic Oncology Group studies. Int J Gynecol Pathol. 1994;13(2):99-108.

[61] Bray, F., Ferlay, J., Soerjomataram, I., Siegel, R. L., Torre, L. A., & Jemal, A. (2018). Global cancer statistics 2018: GLOBOCAN estimates of incidence and mortality worldwide for 36 cancers in 185 countries. *CA: a cancer journal for clinicians*, *68*(6), 394-424.

[62] Bedell, S. L., Goldstein, L. S., Goldstein, A. R., & Goldstein, A. T. (2019). Cervical Cancer Screening: Past, Present, and Future. *Sexual Medicine Reviews*.

[63] Livingston, J., & Papagiannakis, E. (2016). How colposcopy misses invasive cervical cancer: a case report from the IMPROVE-COLPO study. *Case reports in obstetrics and gynecology*, *2016*.

[64] Zhang, T., Luo, Y. M., Li, P., Liu, P. Z., Du, Y. Z., Sun, P., ... & Xue, H. (2020). Cervical precancerous lesions classification using pre-trained densely connected convolutional networks with colposcopy images. *Biomedical Signal Processing and Control*, *55*, 101566

[65] Mayor, S. (2016). Screening reduced cervical cancer deaths by more than two thirds, UK study finds.

[66] Dickinson, J. A., Stankiewicz, A., Popadiuk, C., Pogany, L., Onysko, J., & Miller, A. B. (2012). Reduced cervical cancer incidence and mortality in Canada: national data from 1932 to 2006. *BMC public health*, *12*(1), 992.

[67] Hu, K., Wang, W., Liu, X., Meng, Q., & Zhang, F. (2018). Comparison of treatment outcomes between squamous cell carcinoma and adenocarcinoma of cervix after definitive radiotherapy or concurrent chemoradiotherapy. *Radiation Oncology*, *13*(1), 249.

[68] Zaorsky, N. G., & Horwitz, E. M. (2016). Brachytherapy for Prostate Cancer: An Overview. In *Prostate Cancer* (pp. 399-411). Academic Press.

[69] Han, K., Milosevic, M., Fyles, A., Pintilie, M., & Viswanathan, A. N. (2013). Trends in the utilization of brachytherapy in cervical cancer in the United States. *International Journal of Radiation Oncology* Biology* Physics*, *87*(1), 111-119.

[70] Viswanathan, A. N., Beriwal, S., Jennifer, F., Demanes, D. J., Gaffney, D., Hansen, J., ... & Erickson, B. (2012). American Brachytherapy Society consensus guidelines for locally advanced carcinoma of the cervix. Part II: high-dose-rate brachytherapy. *Brachytherapy*, *11*(1), 47-52.

[71] Karlsson, J., Dreifaldt, A. C., Mordhorst, L. B., & Sorbe, B. (2017). Differences in outcome for cervical cancer patients treated with or without brachytherapy. *Brachytherapy*, *16*(1), 133-140.

[72] Rose, P. G., Bundy, B. N., Watkins, E. B., Thigpen, J. T., Deppe, G., Maiman, M. A., ... & Insalaco, S. (1999). Concurrent cisplatin-based radiotherapy and chemotherapy for locally advanced cervical cancer. *New England Journal of Medicine*, *340*(15), 1144-1153.

[73] Fokdal, L., Sturdza, A., Mazeron, R., Haie-Meder, C., Tan, L. T., Gillham, C., ... & Pötter, R. (2016). Image guided adaptive brachytherapy with combined intracavitary and interstitial technique improves the therapeutic ratio in locally advanced cervical cancer: Analysis from the retroEMBRACE study. *Radiotherapy and Oncology*, *120*(3), 434-440.

[74] Rijkmans, E. C., Nout, R. A., Rutten, I. H. H. M., Ketelaars, M., Neelis, K. J., Laman, M. S., ... & Creutzberg, C. L. (2014). Improved survival of patients with cervical cancer treated with image-guided brachytherapy compared with conventional brachytherapy. *Gynecologic oncology*, *135*(2), 231-238.

[75] Pötter, R., Dimopoulos, J., Georg, P., Lang, S., Waldhäusl, C., Wachter-Gerstner, N., ... & Kirisits, C. (2007). Clinical impact of MRI assisted dose volume adaptation and dose escalation in brachytherapy of locally advanced cervix cancer. *Radiotherapy and oncology*, *83*(2), 148-155.

[76] Holschneider, C. H., Petereit, D. G., Chu, C., Hsu, I. C., Ioffe, Y. J., Klopp, A. H., ... & Yashar, C. (2019). Brachytherapy: A critical component of primary radiation therapy for cervical cancer: For the Society of Gynecologic Oncology (SGO) and the American Brachytherapy Society (ABS). *Brachytherapy*.

[77] Funk, R. K., Stockham, A. L., & Issa Laack, N. N. (2016). Chapter 3 - Basics of Radiation Therapy. *Clinical Cardio-Oncology*. 39-60.

[78] Mendez, L. C., Weiss, Y., D'Souza, D., Ravi, A., Barbera, L., & Leung, E. (2017). Three-dimensional-guided perineal-based interstitial brachytherapy in cervical cancer: A systematic review of technique, local control and toxicities. *Radiotherapy and Oncology*, *123*(2), 312-318.

[79] Tan, P. W., Koh, V. Y., & Tang, J. I. (2015). Outpatient combined intracavitary and interstitial cervical brachytherapy: barriers and solutions to implementation of a successful programme–a single institutional experience. *Journal of contemporary brachytherapy*, *7*(3), 259.

[80] Rodgers, J. R., Surry, K., Leung, E., D'Souza, D., & Fenster, A. (2017). Toward a 3D transrectal ultrasound system for verification of needle placement during high-dose-rate interstitial gynecologic brachytherapy. *Medical physics*, *44*(5), 1899-1911.

[81] Castelnau-Marchand, P., Chargari, C., Haie-Meder, C., & Mazeron, R. (2016). Image-guided adaptive brachytherapy in locally advanced cervical cancer: recent advances and perspectives. *Current opinion in oncology*, *28*(5), 419-428.

[82] Skliarenko, J., Carlone, M., Tanderup, K., Han, K., Beiki-Ardakani, A., Borg, J., ... & Ujaimi, R. (2018). Technique adaptation, strategic replanning, and team learning during implementation of MR-guided brachytherapy for cervical cancer. *Brachytherapy*, *17*(1), 86-93.

[83] Fields, E. C., Hazell, S., Morcos, M., Schmidt, E. J., Chargari, C., & Viswanathan, A. N.

(2020, January). Image-Guided Gynecologic Brachytherapy for Cervical Cancer. In *Seminars in radiation oncology* (Vol. 30, No. 1, pp. 16-28). WB Saunders.

[84] Fokdal, L., Tanderup, K., Hokland, S. B., Røhl, L., Pedersen, E. M., Nielsen, S. K., ... & Lindegaard, J. C. (2013). Clinical feasibility of combined intracavitary/interstitial brachytherapy in locally advanced cervical cancer employing MRI with a tandem/ring applicator in situ and virtual preplanning of the interstitial component. *Radiotherapy and Oncology*, *107*(1), 63-68.

[85] Tiwari, R., Narayanan, G. S., Narayanan, S., & Kumar, P. S. (2019). Long-term effectiveness and safety of image-based, transperineal combined intracavitary and interstitial brachytherapy in treatment of locally advanced cervical cancer. *Brachytherapy*.

[86] Murakami, N., Kobayashi, K., Kato, T., Nakamura, S., Wakita, A., Okamoto, H., ... & Takahashi, K. (2016). The role of interstitial brachytherapy in the management of primary radiation therapy for uterine cervical cancer. *Journal of contemporary brachytherapy*, *8*(5), 391.

[87] Lee, S., Rodney, E., Traughber, B., Biswas, T., Colussi, V., & Podder, T. (2017). Evaluation of interfractional variation of organs and displacement of catheters during high-dose-rate interstitial brachytherapy for gynecologic malignancies. *Brachytherapy*, *16*(6), 1192-1198.

[88] Otter, S., Coates, A., Franklin, A., Cunningham, M., & Stewart, A. (2018). Improving dose delivery by adding interstitial catheters to fixed geometry applicators in high-dose-rate brachytherapy for cervical cancer. *Brachytherapy*, *17*(3), 580-586.

[89] Fallon, J., Park, S. J., Yang, L., Veruttipong, D., Zhang, M., Van, T., ... & Steinberg, M. L. (2017). Long term results from a prospective database on high dose rate (HDR) interstitial brachytherapy for primary cervical carcinoma. *Gynecologic oncology*, *144*(1), 21-27.

[90] Liu, Z. S., Guo, J., Zhao, Y. Z., Lin, X., Zhang, B. Y., Zhang, C., ... & Wang, T. J. (2017). Computed Tomography–Guided Interstitial Brachytherapy for Locally Advanced Cervical

Cancer: Introduction of the Technique and a Comparison of Dosimetry With Conventional Intracavitary Brachytherapy. *International Journal of Gynecologic Cancer*, *27*(4), 768-775.

[91] Tan, L. T., de Leeuw PhD, A., Schmid, M., Haie-Meder, C., Mahantshetty, U., DM, J. C. L., & Pötter, R. (2019, July). Image-guided adaptive radiotherapy in cervical cancer. In *Seminars in radiation oncology* (Vol. 29, No. 3, pp. 284-298). WB Saunders.

[92] Jaeger, H. A., Franz, A. M., O'Donoghue, K., Seitel, A., Trauzettel, F., Maier-Hein, L., & Cantillon-Murphy, P. (2017). Anser EMT: the first open-source electromagnetic tracking platform for image-guided interventions. *International journal of computer assisted radiology and surgery*, *12*(6), 1059-1067.

[93] Xie, J., Qin, C., Zhou, X., Huang, L., Han, X., Wang, M., & Li, L. (2013). The simulations and experiments of the electromagnetic tracking system based on magnetic dipole model. *IEEE transactions on applied superconductivity*, *24*(3), 1-4.

[94] Franz, A. M., Haidegger, T., Birkfellner, W., Cleary, K., Peters, T. M., & Maier-Hein, L. (2014). Electromagnetic tracking in medicine—a review of technology, validation, and applications. *IEEE transactions on medical imaging*, *33*(8), 1702-1725.

[95] Sadjadi, H., Hashtrudi-Zaad, K., & Fichtinger, G. (2015). Simultaneous electromagnetic tracking and calibration for dynamic field distortion compensation. *IEEE Transactions on Biomedical Engineering*, *63*(8), 1771-1781.

[96] Maier-Hein, L., Franz, A. M., Birkfellner, W., Hummel, J., Gergel, I., Wegner, I., & Meinzer, H. P. (2012). Standardized assessment of new electromagnetic field generators in an interventional radiology setting. *Medical physics*, *39*(6Part1), 3424-3434.

[97] Jaeger, H. A., Hinds, S., & Cantillon-Murphy, P. (2018, September). An open framework enabling electromagnetic tracking in image-guided interventions. In *International Conference on Medical Image Computing and Computer-Assisted Intervention* (pp. 168-175). Springer, Cham.

[98] Anser design repository. https://osf.io/47q8q/. Accessed on 01/23/2020.

[99] O'Donoghue, K., Eustace, D., Griffiths, J., O'Shea, M., Power, T., Mansfield, H., & Cantillon-Murphy, P. (2014). Catheter position tracking system using planar magnetics and closed loop current control. *IEEE transactions on magnetics*, *50*(7), 1-9.

[100] O'Donoghue, K., & Cantillon-Murphy, P. (2014). Low cost super-Nyquist asynchronous demodulation for use in EM tracking systems. *IEEE Transactions on Instrumentation and Measurement*, *64*(2), 458-466.

[101] González-Landaeta, R., Cota-Ruiz, J., Sifuentes, E., Díaz, J., & Casas, O. (2019). A Fully Differential Synchronous Demodulator for AC Signals. *IEEE Transactions on Instrumentation and Measurement*, *69*(1), 35-44.

[102] Andria, G., Attivissimo, F., Di Nisio, A., Lanzolla, A. M. L., Larizza, P., & Selicato, S. (2019). Development and performance evaluation of an electromagnetic tracking system for surgery navigation. *Measurement*, *148*, 106916.

[103] Zhou, J., Zamdborg, L., & Sebastian, E. (2015). Review of advanced catheter technologies in radiation oncology brachytherapy procedures. *Cancer management and research*, *7*, 199.

[104] Chen, Y., Wang, W., Schmidt, E. J., Kwok, K. W., Viswanathan, A. N., Cormack, R., & Tse, Z. T. H. (2015). Design and fabrication of MR-tracked metallic stylet for gynecologic brachytherapy. *IEEE/ASME Transactions on Mechatronics*, *21*(2), 956-962.

[105] Garg, A., Patil, S., Siauw, T., Cunha, J. A. M., Hsu, I. C., Abbeel, P., ... & Goldberg, K. (2013, August). An algorithm for computing customized 3D printed implants with curvature constrained channels for enhancing intracavitary brachytherapy radiation delivery. In *2013 IEEE International Conference on Automation Science and Engineering (CASE)* (pp. 466-473). IEEE.

[106] Pernelle, G., Mehrtash, A., Barber, L., Damato, A., Wang, W., Seethamraju, R. T., ... &

Kapur, T. (2013, September). Validation of catheter segmentation for MR-guided gynecologic cancer brachytherapy. In *International Conference on Medical Image Computing and Computer-Assisted Intervention* (pp. 380-387). Springer, Berlin, Heidelberg.

[107] Ercegovac, M. D., Lang, T. (2004).CHAPTER 4 - Multiplication, In *The Morgan Kaufmann Series in Computer Architecture and Design* (pp 180-245). https://doi.org/10.1016/B978-155860798-9/50006-3. Digital Arithmetic, Morgan Kaufmann.

[108] Mastmeyer, A., Pernelle, G., Ma, R., Barber, L., & Kapur, T. (2017). Accurate model-based segmentation of gynecologic brachytherapy catheter collections in MRI-images. *Medical image analysis*, *42*, 173-188.

[109] Arabnia, H. R., & Tran, Q. N. (2016). *Emerging trends in applications and infrastructures for computational biology, bioinformatics, and systems biology: systems and applications*. Morgan Kaufmann.

[110] Kirisits, C., Rivard, M. J., Baltas, D., Ballester, F., De Brabandere, M., van der Laarse, R., ... & Tanderup, K. (2014). Review of clinical brachytherapy uncertainties: analysis guidelines of GEC-ESTRO and the AAPM. *Radiotherapy and oncology*, *110*(1), 199-212.

[111] Damato, A. L., Cormack, R. A., & Viswanathan, A. N. (2014). Characterization of implant displacement and deformation in gynecologic interstitial brachytherapy. *Brachytherapy*, *13*(1), 100-109.

[112] Shaaer, A., Davidson, M., Semple, M., Nicolae, A., Mendez, L. C., Chung, H., ... & Ravi, A. (2019). Clinical evaluation of an MRI-to-ultrasound deformable image registration algorithm for prostate brachytherapy. *Brachytherapy*, *18*(1), 95-102.

[113] Guthier, C. V., Damato, A. L., Hesser, J. W., Viswanathan, A. N., & Cormack, R. A. (2017). A fast inverse treatment planning strategy facilitating optimized catheter selection in image-guided high-dose-rate interstitial gynecologic brachytherapy. *Medical physics*, *44*(12), 6117-6127.

[114] Wu, J., Liu, M., Zhou, Z., & Li, R. (2018). Fast Rigid 3D Registration Solution: A Simple Method Free of SVD and Eigen-Decomposition. *arXiv preprint arXiv:1806.00627*

[115] Götz, T. I., Lahmer, G., Strnad, V., Bert, C., Hensel, B., Tomé, A. M., & Lang, E. W. (2017). A tool to automatically analyze electromagnetic tracking data from high dose rate brachytherapy of breast cancer patients. *PloS one*, *12*(9).

[116] Tanderup, K., Fokdal, L. U., Sturdza, A., Haie-Meder, C., Mazeron, R., Van Limbergen, E., ... & Bentzen, S. M. (2016). Effect of tumor dose, volume and overall treatment time on local control after radiochemotherapy including MRI guided brachytherapy of locally advanced cervical cancer. *Radiotherapy and Oncology*, *120*(3), 441-446.

[117] Attivissimo, F., Lanzolla, A. M. L., Carlone, S., Larizza, P., & Brunetti, G. (2017, May). TDM-FDM configuration of electromagnetic tracking system for image-guided surgery devices. In *2017 IEEE International Instrumentation and Measurement Technology Conference (I2MTC)* (pp. 1-6). IEEE.

[118] Li, M., Bien, T., & Rose, G. (2013). FPGA based electromagnetic tracking system for fast catheter navigation. *Int J Sci Eng Res*, *4*(9), 2566-2570.

[119] Higgins F.R., ‘‘AC magnetic tracking with phase disambiguation,’’ U.S. Patent, 2009035645 A1, 2009.

[120] Li, M., Hansen, C., & Rose, G. (2015). A robust electromagnetic tracking system for clinical applications. In *CURAC* (pp. 31-36).

[121] Attivissimo, F., Di Nisio, A., Lanzolla, A. M. L., Selicato, S., & Larizza, P. (2018). Evaluation of noise performance of an electromagnetic image-guided surgery system. Paper presented at the 1-6. doi:10.1109/I2MTC.2018.8409753.

[122] IEEE Standard for Safety Levels with Respect to Human Exposure to Electromagnetic Fields, 0-3 kHz, Std. C95.6-2002.

[123] IEEE Standard for Safety Levels with Respect to Human Exposure to Radio requency Electromagnetic Fields, 3 kHz to 300 GHz, Std. C95.1- 2005, Revision of IEEE Std C95.1 - 1991, 2006.

[124] Bien, T., & Rose, G. (2012, January). Algorithm for calibration of the electromagnetic tracking system. In *Proceedings of 2012 IEEE-EMBS International Conference on Biomedical and Health Informatics* (pp. 85-88). IEEE.

[125] Anser design repository. https://osf.io/47q8q/. Accessed on 02/26/2020

[126] Hinds, S., Jaeger, H. A., Burke, R., O'Sullivan, B., Keane, J., Trauzettel, F., ... & Hofstad, E. F. (2019). An open electromagnetic tracking framework applied to targeted liver tumour ablation. *International journal of computer assisted radiology and surgery*, *14*(9), 1475-1484.

[127] Wronski, M., Leung, E., Davidson, M., & Ravi, A. (2015). Interstitial High-Dose-Rate Gynecological Brachytherapy: Dosimetric Impact of Catheter Deflection. *Brachytherapy*, *14*, S86.

[128] Zhou, J., Sebastian, E., Mangona, V., & Yan, D. (2013). Real-time catheter tracking for high-dose-rate prostate brachytherapy using an electromagnetic 3D-guidance device: a preliminary performance study. *Medical physics*, *40*(2), 021716.

[129] Franz, A. M., März, K., Hummel, J., Birkfellner, W., Bendl, R., Delorme, S., ... & Maier-Hein, L. (2012). Electromagnetic tracking for US-guided interventions: standardized assessment of a new compact field generator. *International journal of computer assisted radiology and surgery*, *7*(6), 813-818.

[130] Mehrtash, A., Damato, A., Pernelle, G., Barber, L., Farhat, N., Viswanathan, A., ... & Kapur, T. (2014, March). EM-navigated catheter placement for gynecologic brachytherapy: an accuracy study. In *Medical Imaging 2014: Image-Guided Procedures, Robotic Interventions, and Modeling* (Vol. 9036, p. 90361F). International Society for Optics and Photonics.

[131] Rodgers, J. R., Bax, J., Surry, K., Velker, V., Leung, E., D'Souza, D., & Fenster, A. (2019). Intraoperative 360-deg three-dimensional transvaginal ultrasound during needle insertions for high-dose-rate transperineal interstitial gynecologic brachytherapy of vaginal tumors. *Journal of Medical Imaging*, *6*(2), 025001.

[132] Viswanathan, A. N., Moughan, J., Small, W., Levenback, C., Iyer, R., Hymes, S., ... & Gaffney, D. K. (2012). The quality of cervical cancer brachytherapy implantation and the impact on local recurrence and disease-free survival in radiation therapy oncology group prospective trials 0116 and 0128. *International Journal of Gynecologic Cancer*, *22*(1), 123-131.

[133] Sethi, R., Kuo, Y. C., Edraki, B., Lerner, D., Paik, D., & Bice, W. (2018). Real-time Doppler ultrasound to identify vessels and guide needle placement for gynecologic interstitial brachytherapy. *Brachytherapy*, *17*(5), 742-746.

[134] Götz, T. I., Lahmer, G., Strnad, V., Bert, C., Hensel, B., Tomé, A. M., & Lang, E. W. (2017). A tool to automatically analyze electromagnetic tracking data from high dose rate brachytherapy of breast cancer patients. *PloS one*, *12*(9).

[135] Masitho, S., Kallis, K., Strnad, V., Fietkau, R., & Bert, C. (2019). Error detection using an electromagnetic tracking system in multi-catheter breast interstitial brachytherapy. *Physics in Medicine & Biology*, *64*(20), 205018.

[136] Kellermeier, M., Fietkau, R., Strnad, V., & Bert, C. (2018). Assessment of the implant geometry in fractionated interstitial HDR breast brachytherapy using an electromagnetic tracking system. *Brachytherapy*, *17*(1), 94-102.

[137] Choi, C. H., Park, S. Y., Park, J. M., Wu, H. G., Kim, J. H., & Kim, J. I. (2018). Comparison of the IPSA and HIPO algorithms for interstitial tongue high-dose-rate brachytherapy. *PloS one*, *13*(10).